



## High-Throughput Image-Guided Microprobe Mass Spectrometric Analysis of Single Cells

Stanislav S. Rubakhin, Elena V. Romanova, and Jonathan V. Sweedler

### Abstract

Characterizing the chemicals within individual cells is an important analytical capability, with mass spectrometry (MS) being one of the most chemically information-rich techniques available. There are two major approaches for characterizing single cells using MS: the assay of small-volume solutions using electrospray ionization and, the focus of this chapter, measurement of cells dispersed across a surface using matrix-assisted laser desorption/ionization (MALDI) MS. In combination with spatiometric information obtained via optical imaging tools to locate individual cells on the sampling surface, follow-up measurement via MALDI MS can profile a multitude of single cells in a high-throughput manner. Compared to conventional MS imaging of the entire sample-containing surface, preselection of accurate cell locations for targeted analysis increases selectivity and throughput as well as reduces overall data size. As a result, more informative data sets are produced in less time with fewer resources. Employing this strategy, we present a multistage protocol for optical image-guided, high-throughput single cell analysis by MALDI MS. We outline steps for the isolation and preparation of single cells prior to dispersing on a glass slide for optical imaging, automated mapping of imaged cell locations using microMS, preparing the cells for MALDI MS analysis using standards and MALDI matrices, acquisition of mass spectra from mapped individual cells, and data processing and statistical analysis. Images obtained via a range of microscopy modalities can be assessed by the microMS custom image processing software suite to determine location coordinates for cells with defined morphological and/or biochemical characteristics. Depending on the biological model and MS instrumentation used, this strategy can be further enhanced by hyphenation of different imaging modalities, e.g., electron microscopy, for multidimensional sample characterization.

**Key words** Single cell, MicroMS, Mass spectrometry, Pancreatic islets, Peptides, Microanalysis, High throughput, Matrix-assisted laser desorption/ionization

---

### 1 Introduction

Arguably, the cell is the most fundamental unit of life and possesses a variety of the needed mechanisms of independent function and replication. Structural similarity among cells is the basis of tissue formation and reproduction of organisms, whereas heterogeneity among similar cells is critical for organism functioning. Since its observation by Robert Hooke [1], the cell has become an

important target of scientific analysis. Improvements in the sensitivity of mass spectrometry (MS) now enable single cell and subcellular analysis, allowing us to obtain unique multiplexed chemical information on the presence of inorganic compounds, metabolites, lipids, peptides, proteins, oligonucleotides, and polynucleotides in single cells. A variety of MS approaches have been adapted to single cell analysis, with secondary ionization mass spectrometry (SIMS), electrospray ionization (ESI)-MS, and matrix-assisted laser desorption/ionization (MALDI) MS being most frequently used. Each of these approaches has advantages and disadvantages, including specific requirements for sample handling and analyte extraction.

The goals of bioanalytical single cell MS are often the detection and structural and quantitative characterization of endogenous and exogenous compounds. The multiplexed nature of MS analysis permits coverage of a wide range of analyte classes, making the detection and characterization of important components of the metallome, metabolome, lipidome, peptidome, and proteome of a cell possible [2, 3]. Due to normal and pathological variabilities and heterogeneities of biological systems, often exacerbated by sample handling during preparation, experimental success depends on the analysis of a representative number of samples (replicates) to provide sufficient statistical power. As even a small sample can contain hundreds of thousands to millions of cells, such MS measurements may consume unrealistic resources and time. Therefore, optimization of data collection leads to more efficient measurements, enhanced results, and reduced data size. Though one can reduce the amount of data obtained and enhance analyses using several post-acquisition approaches, here we present a protocol that improves data acquisition time and efficiency during the sample preparation and optical imaging stages to facilitate high-throughput single cell MALDI MS analysis. An important component of this approach is the ability to filter individual cells with predetermined morphometric and biochemical characteristics and only select specific cells for follow-up MS analysis, excluding empty spaces and structures, such as debris and dust. We have optimized this protocol for the analysis of low-density populations of individual cells dispersed across a glass slide, which is a common practice in biomedical investigations and clinical applications.

### **1.1 Comparison with Other Approaches**

Image analysis approaches have widespread application in a variety of sample characterization processes, including single cell recognition, characterization, and identification [4–7]. More broadly, optical information for object location and sorting is widely used in diverse applications, from fluorescent cell sorting [8, 9] to industrial applications of computer vision systems [10], manufacturing quality controls [11, 12], biomedical fields [13, 14], and big data-related analyses [15].

For spatial information-guided MS of single cells, two approaches are typically used: (1) operator-defined targeting of a region of interest within the sample and (2) analysis of samples deposited at predefined coordinates. The first approach is widely used in mass spectrometry imaging (MSI) where measurements are typically performed on manually selected areas having the desired morphological features, such as defined brain regions on brain slices. Measurement of systematically deposited single cells (e.g., into array patterns), including individual bacteria, has been effective with MS-based approaches, e.g., microarrays for mass spectrometry (MAMS) [16–18], cell sorting with surface deposition [19], and cell culture MS analysis [20, 21]. These cell targeting approaches have multiple benefits, including high methodological control in the sample localization process; however, they have some limitations. For example, MAMS requires specifically designed and manufactured wells (tailored to the size of the cells) that may complicate work with cellular populations of different cell sizes, such as populations of isolated hippocampal neurons having more than 100- $\mu\text{m}$ -long terminals. For MSI, information is acquired on all spots in a sample, some of which are empty spaces, nonbiological structures, and cells. As result, a lower measurement throughput is achieved and larger data files are created. Moreover, because cellular debris will also be measured, the data set will require greater post-processing effort.

Also interesting are the flow-based MS approaches, which can quickly analyze hundreds to tens of thousands of individual cells delivered to the mass spectrometer in a continuous flow of solution. For example, mass cytometry utilizes fast, orderly delivery of cells and sampling of their chemical composition using an inductively coupled argon plasma (ICP) [22]. Moving away from MS, several spectroscopic methods may provide multiplexed chemical information from single cell populations including direct measurements by Raman Fourier transform (FT) spectroscopy [23], infrared spectroscopy [24], and affinity probe-based methods, such as sequential multiplex staining of cells and tissues [25, 26] targeting multiple analyte classes that is dependent on probe specificity.

## **1.2 Development of the Approach**

Several decades of work [27–29] on the development and application of single cell MALDI MS have demonstrated its ability to aid in the discovery of new neuropeptides in selected cells. While the approach is effective when specific cells need to be assayed, throughput has been a major bottleneck, limiting MALDI MS analysis to small numbers of individual cells. To address this issue, we increased throughput by placing low-density scattered cells on a slide, locating their positions, and then using these positions to guide the laser (or ion beam for SIMS) [30–32]. Because this process was somewhat tedious, in 2017 our group developed the software package *microMS* [33] to automate cell finding and

improve coordinate registration via a user-friendly GUI interface, and using point-based image registration to correlate fiducial markers on the microscopy image to physical coordinates on the mass spectrometer's stage. The targeted profiling steps enabled by the microMS-guided workflow include the ability to (1) determine locations/coordinates of cells or other structures dispersed across a microscope slide using an optical image; (2) select coordinates of subpopulations of detected features (e.g., cells) according to flexible, user-defined criteria, such as shape and intercellular distances; and (3) convert the cell pixel coordinates to physical stage coordinates for the measurement platform (i.e., mass spectrometer) being used. Importantly, the positional information can be combined with other analyses, such as post-MALDI MS selected cell sampling and capillary electrophoresis (CE)-MS analysis [34]. While developed for single cell analysis, with modifications the underlying microMS code is versatile and can be applied to a variety of samples, imaging modalities, and chemical analysis techniques. For more advanced users, the addition of new, off-line instrument platforms and even direct instrument control is possible. We describe the most common usage of microMS, detail additional features, and provide a starting point for its application to a range of other platforms. Preparing the biological samples and performing the MS measurements require a medium level of expertise. Our experience with training undergraduate research assistants has shown us that novice users are capable of producing repeatable results after 2–3 months of practice, and this is the audience aimed for here. A higher level of expertise or additional expert advice may be needed for tissues that are hard to dissociate or when using complex or unusual MS equipment.

### **1.3 Overview of the Approach**

The combination of single cell isolation, single cell MS, optical imaging, optical image processing utilities, and molecular probes provides opportunities for cell chemical typing and determination of the chemical stability and heterogeneity of cell types in larger cellular populations. Though such combined measurements are not common, the key mass spectrometric and optical imaging hardware and software already exist, enabling us to link these approaches together using the integrative microMS software package.

The major methodological steps in this multistage protocol are (1) biological sample preparation, to include dissociation of individual cells via enzymatic and/or mechanical treatments, labeling with fluorescent dye, and deposition of cells onto an ITO-coated glass slide and stabilized with glycerol, followed by partial or complete glycerol removal using washing buffers; (2) acquisition of an optical image of cells under fluorescent and transmitted light; (3) processing of the acquired image with microMS to determine cell location coordinates according to user-defined criteria; (4) sample preparation for MALDI MS analysis consisting of analyte

standard deposition and MALDI matrix application (after this stage, samples can be stored at low temperatures in a desiccator or in a low oxygen environment but should be acclimated to ambient temperature before MS analysis); (5) loading of the sample into a mass spectrometer and performing point-based image registration by locating fiducial markers in microMS and the same location on the MS stage; (6) loading coordinates of the targeted cells into the mass spectrometer's software; (7) acquisition of mass spectra; (8) and finally, data processing and analyses using a variety of computational tools available from different industrial and academic sources. The main goals of the analyses are the measurement of the chemistry within the cell, thus enabling chemical heterogeneity of cellular populations to be probed, and the biomarkers for cell types to be determined.

Using this approach, several hundred to a thousand cells per slide are commonly measured. Depending on the instrument used and settings selected, each slide can be analyzed in less than 1 hour, allowing at least eight slides to be processed per day. There are several options for further increasing the number of analyzed slides, including automation of sample loading/unloading as well as generation of scripts for automatic import of cell coordinates and instrument training (e.g., mass spectrometer) using preset fiducial marks, and available hardware and software. However, additional efforts should be made toward registration of fiducial marks after sample loading into a mass spectrometer. This step currently requires involvement of an operator and thus, limits measurements to operator availability.

#### ***1.4 Advantages and Disadvantages of the Approach***

Analysis of intact cells provides distinct advantages in comparison with MS measurements of thin tissue sections. In most cases, tissue section samples analyzed with MS do not provide information on the chemical profile of individual cells. This may be because cells are cross-sectioned and only parts of cells are analyzed, or interference from other surrounding cells is causing difficulties in assessing cell content. In addition, even when the probe size is on the order of (or smaller than) a cell, cells are irregularly shaped and the probes are often not well-aligned with cells, so that one is not assured of sampling from an individual cell when assaying tissue sections.

In contrast, dispersing individual cells at distances typically exceeding the probe (laser) diameter ensures that different cells are not examined simultaneously. In addition, one can use wetter conditions for analyte extraction and incorporation into MALDI matrix crystals so that limited spreading of the analytes to adjacent sections is not an issue. Because of these factors, single cell MALDI MS increases data reliability by reducing single cell sample cross-contamination and decreases the likelihood that noncellular structures or multicellular aggregates are assayed. The microMS-based workflow can be adapted to a large variety of sample plates besides

the standard microscopy glass slide. Fluorescent images can also be taken from nontransparent, 386-well polished MALDI sample plates and custom-designed glass or silicon sample plates [35]. Optical image-guided MS analysis can be adapted to other imaging modalities, including electron microscopy, and magnetic resonance, x-ray, and ultrasound imaging. As a last benefit of MALDI MS, after a measurement, much of the sample is left, allowing the remaining material to be characterized again. We already have demonstrated that several technologies can be combined with microMS-based analysis for single cell measurements, including CE-MS [34] and immunolabeling [36], and it is likely that others will follow.

As with many other technologies for measuring single cells, there are some limitations to the described approach, but there are also viable solutions to overcoming some of these challenges. microMS-based single cell MS analysis does not preserve information on intra-specimen localization of individual cells within a sampled tissue. To correlate single cell and tissue level data sets with cell type/state, biomarkers can be used in follow-up measurements of the same tissue utilizing MSI or immunohistochemistry, thereby addressing this issue. Another concern is that bias can be introduced when isolating cells because of differences in their mechanical stability or susceptibility to damage during dissociation. If one cell type is damaged and another is not, this would be difficult to determine based solely on the MS data. Moreover, different enzymatic treatments may be needed for isolation of astrocytes and neurons, or cells may not be stained uniformly with a specific dye. For example, we have noticed that Hoechst 33342 produces dim staining in cerebellar Purkinje neurons compared to granular cells. As a remedy, the addition of dyes for monitoring cell pyroptosis, apoptosis, or cell lysis [37], followed by optical imaging and exclusion of specific cells during MS analysis, can be introduced.

Despite the multiplexed nature of single cell MALDI MS analysis, analyte coverage is relatively low, typically with 10–200 compounds detected. This issue is due in part to low analyte amounts and also because of the relatively low dynamic range and resolving power of direct MS compared to hyphenated approaches such as CE-MS and liquid chromatography (LC)-MS. However, the introduction of ion mobility to the front end should address this drawback, and use of ultrahigh-resolution FTMS should also increase the number of analytes detected and characterized.

Despite the limitations noted above, microMS-based single cell MS is a flexible and versatile platform for analyses of cellular agglomerates and single cells that we have successfully applied to the characterization of cellular populations of individual islets of Langerhans, dorsal root ganglia, and brain regions [32, 36, 38]. Low analyte consumption techniques, such as SIMS and

MALDI MS, are hyphenated for analysis of the same cellular population and provide wider analyte coverage and additional opportunities for cell phenotyping [38]. Low analyte consumption as well as characteristic sample preparation for MALDI MS, where not all analytes are extracted and incorporated into MALDI matrix crystals, allows post-MALDI MS detection of cellular proteins using immunolabeling [36] and metabolites by CE hyphenated to ESI-MS [34]. microMS is critical for determining cell targets for more time-consuming analytical measurements such as CE ESI-MS. Typically, a single CE ESI-MS run takes 10–30 min; therefore, only a small number of cells can be analyzed. MALDI MS provides information on cell content and cell types to guide selection of single cells for a follow-up analysis by CE-MS. microMS processing of coordinates of cellular locations enables different approaches for cell content collection, including micro-junction approaches as well as other analytical platforms [34].

While more standard applications of the approach are covered here, microMS can be tailored to new and diverse instruments and also offers more advanced operations, including direct instrument control. For example, many other types of single cell analysis can be hyphenated with microMS, e.g., vibrational spectroscopies such as infrared, near infrared, and Raman. Knowledge of cell coordinates allows formation of multiplatform data sets for extensive characterization of individual cells and cellular populations. Single organelle analysis is a new area for microMS-based MS [39]; however, this application is not covered in the current protocol.

### **1.5 Experimental Design Considerations**

It is important to ensure that all components of the experimental design are compatible and sufficiently flexible for achieving the planned goals. For example, not all instrumental software packages are capable of generating optical image files that are compatible with microMS. Also, some cell labeling methods may not be equally efficient for specific cell types. Depending on the biological model, targeted analyte class, and study goals, different approaches have to be chosen for different stages of the experimental process, beginning with suitable cell isolation, labeling and storage techniques, selection of the MALDI matrix, and microscopy and MS instrumentation, and finally, choosing appropriate data analysis tools, methods, and resources.

Especially important is the quality of the cell isolation and sample preparation process to ensure accurate representation of the cell population. All components should be tested at the preliminary stage of planning. Before the actual experiment is started, multiple optimizations should be implemented and evaluated for the analytes of interest, e.g., dispersing cells at an appropriate cell density, optimizing the MALDI matrix solution and its application, and adjusting the MALDI MS parameters. All solutions and surfaces used should be tested for the presence of detectable, or not

detectable but interfering, analytes and compounds. For example, polymers such as polyethylene glycol and polysiloxane are often used in molecular biology but cannot be used for this protocol. Therefore, control experiments utilizing analyte standards and well-characterized biological models should be performed.

In cases of long-term studies where samples become available over an extended time, the timing and order of their analysis should be considered. MS of biological samples is prone to batch effects; therefore, accumulation of samples and their appropriate storage must be validated in a relatively short period of time prior to analysis. To further reduce the influence of batch effects, deposition of cell populations collected from different donors on different marked areas of the same glass slide in random order is suggested.

---

## 2 Materials

### 2.1 *Biological Materials*

When developing this protocol, we used cells from the rat and human islets of Langerhans as models. Isolated human islets were provided by our collaborators at the University of Pennsylvania, with the sample collection and processing approved by the University of Pennsylvania Institutional Review Board (protocol number: 832134). Written consent was obtained from responsible parties (tissue donors or relatives of donors). The handling of human cell samples was performed in accordance with Biosafety Level 2 regulations described for the project and approved by the relevant Institutional Biosafety Committees. Adult Sprague-Dawley rats were purchased from ENVIGO (<https://www.envigo.com/model/hsd-sprague-dawley-sd>). Protocols for animal care and procedures were approved by an Institutional Animal Care and Use Committee and be in full compliance with local, federal, and some international guidelines for the humane care and treatment of animals.

### 2.2 *Reagents*

1. 2,5-Dihydrobenzoic acid (DHB) (MilliporeSigma, cat. no. A3539).
2. 4-(2-Hydroxyethyl)piperazine-1-ethanesulfonic acid (HEPES) (MilliporeSigma, cat. no. H3375).
3. Acetonitrile (ACN) (Thermo Fisher Scientific, cat. no. A998-4).  
!CAUTION ACN is toxic. When handling, wear gloves and use a pipetting aid.
4. Calcium chloride (MilliporeSigma, cat. no. C7902).
5. Glycerol (MilliporeSigma, cat. no. G7893).
6. Magnesium chloride hexahydrate (MilliporeSigma, cat. no. M2393).



7. Magnesium sulfate heptahydrate (MilliporeSigma, cat. no. M2773).
8. Peptide calibration standard II (angiotensin II, angiotensin I, substance P, bombesin, ACTH clip 1–17, ACTH clip 18–39, somatostatin 28, bradykinin fragment 1–7, renin substrate tetradecapeptide porcine) (Bruker Corp., part no. 222570).
9. Potassium chloride (MilliporeSigma, cat. no. P5405).
10. Potassium phosphate monobasic (MilliporeSigma, cat. no. P5655).
11. Sodium bicarbonate (MilliporeSigma, cat. no. S5761).
12. Sodium chloride (MilliporeSigma, cat. no. S5886).
13. Sodium phosphate (Thermo Fisher Scientific, cat. no. S374–500).
14. Nuclear dye Hoechst 33342 (Thermo Fisher Scientific, cat. no. 62249).
15. Trifluoroacetic acid (TFA) (MilliporeSigma, cat. no. T6508).  
!CAUTION TFA is highly corrosive. When handling, wear gloves and goggles, use a pipetting aid, and operate in a ventilated chemical hood.
16. Trypsin LE (Thermo Fisher Scientific, cat. no. 12604013).
17. Paraformaldehyde (Fisher Scientific, cat. no. 50-980-487).
18. Tris-EDTA buffer solution (Sigma-Aldrich, cat. no. 93283).
19. N-Acetyl-L-cysteine NAC (Sigma-Aldrich, cat. no. A7250).
20. Collagenase P from *Clostridium histolyticum* (Sigma-Aldrich, cat. no. 11213857001).

### **2.3 Laboratory Equipment**

1. Diamond scribe (e.g., Electron Microscopy Sciences, cat. no. 62107-ST).
2. Microtubes, 1.5 mL (e.g., Eppendorf Safe-Lock Tubes, cat. no. 022363204).
3. 15 ml screw-cap tubes (Falcon, cat. no. 352095).
4. 50 ml screw-cap tubes (Falcon, cat. no. 352070).
5. Disposable borosilicate glass Pasteur pipets (Fisher Scientific, cat no. 13–678-20A).
6. Non-treated culture dishes D × H 60 mm × 15 mm (e.g., Corning, cat. no. CLS430589).
7. Disposable safety gloves (e.g., Microflex® 93–833, XCEED® nitrile gloves, powder-free (MilliporeSigma, cat. no. Z687448)).
8. Disposable graduated transfer pipets (e.g., Fisher Scientific, cat. no.13–711-9 AM).

9. Safety glasses (e.g., MR0111ID Mirage safety glasses (Radians, cat. no. MR0111ID).
10. Face masks (e.g., disposable PPE Latex-Free 3-Ply Face Masks, ProPac, SKU: D8012).
11. Paper absorbent wipes (e.g., Kimwipes, Kimberly-Clark Inc., cat. no. 34155).
12. Indium tin oxide (ITO)-coated microscopy glass slides (coating resistance, 70–100 ohms; dimensions, 25 × 75 × 0.8 mm) (e.g., Delta Technologies, cat. No. CG-90IN-S110).
13. Automated matrix spraying system (e.g., HTX M5 Sprayer; HTX Technologies).
14. Water bath for 34–37 °C incubations (Cole-Parmer Polystat EW-20873-45).
15. Digital multimeter – ohmmeter (e.g., HHM10-20-30-DMM-Series, [www.omega.com](http://www.omega.com)).
16. Plastic rectangle microscope glass holders (boxes for five slides).
17. Ultra-microbalance (e.g., Cubis II, Sartorius).
18. Vacuum-sublimation apparatus (e.g., Ace complete apparatus, H × I.D. 250 mm × 152 mm, Sigma-Aldrich, cat. no. Z258717).  
!CAUTION Working with glass vessels kept under vacuum requires establishing and following specific standard operating procedure(s).
19. A Styrofoam box to hold ice
20. pH meter (e.g., FiveEasy Plus pH meter FP20-Micro-Kit, Mettler Toledo, material no. 30266940).
21. Surgical tools, including forceps, scissors, and a vessel clamp (e.g., Fine Science Tools, cat. no. 18320-11).
22. 5 mL plastic syringe with blunt end 20G–30G needle attached. Needle size depends on animal size, to correspond to the diameter of the bile duct, and should be determined experimentally. For easier operation, a fine Teflon or other plastic tubing can be attached to end of needle extending working distance and reducing effect of syringe motion on success of solution injection.
23. Guillotine for rodents (e.g., Nemi Guillotine, Braintree Scientific, cat. no. NS-80 2).
24. Interchangeable magnifier headset with LED used during surgical procedures (e.g., Fine Science Tools, cat. no. 28080-10).
25. Flexible plastic tubing (e.g., Tygon one WHATMAN Inline Filter Device, 60 psi (<https://www.grainger.com/>, item no. 32HK77)).

26. Two 50 mL heavy wall glass filtering flasks (e.g., <https://www.usplastic.com/>, item no. 76984).

#### **2.4 Mass Spectrometry Instruments and Software**

1. MALDI-TOF/TOF mass spectrometer (we use an ultrafleX-treme, Bruker Corp.)
2. Fourier transform ion cyclotron resonance (FTICR) mass spectrometer (we use a 7 T solariX, Bruker Corp.).
3. flexAnalysis software (Bruker Corp.).
4. flexControl software (Bruker Corp.).
5. flexImaging software (Bruker Corp.).

#### **2.5 microMS Software and Hardware**

1. The microMS software downloads (<http://neuroproteomics.scs.illinois.edu/microMS.htm>) are comprised of a compiled Windows executable, “microMS.exe” (ZIP folder), which includes a Python interpreter and all dependencies, and the Python Source Code, “microMS” (ZIP folder). The microMS User Guide can also be downloaded from this site. The operation and use of this code have been described in <https://github.com/troycomi/microMS> and [33].
2. Python (<https://www.python.org/downloads/>).
3. PyQt5 (<https://www.riverbankcomputing.com/software/pyqt/download5>).
4. NumPy (<http://www.numpy.org/>).
5. SciPy (<https://www.scipy.org/>).
6. Matplotlib (<http://matplotlib.org/>).
7. Skimage (<http://scikit-image.org/docs/dev/api/skimage.html>).
8. OpenSlide (<http://openslide.org/>) and OpenSlide Python (<https://github.com/openslide/openslide-python#installation>).
9. PySerial (<https://pypi.python.org/pypi/pyserial>).
10. The software requires a workstation running an up-to-date Windows operating system (e.g., Windows 10, 32 GB of RAM, a 1 TB hard drive), or Linux distributions (e.g., Fedora, Ubuntu).

#### **2.6 Biochemical and Mass Spectrometry Databases**

1. Lipids Maps Structure Database (<http://www.lipidmaps.org/data/structure/>).
2. UniProt (<https://www.uniprot.org>) [39].
3. Human Metabolome Database (<https://hmdb.ca>).
4. MassBank of North America (MoNA) (<https://mona.fiehnlab.ucdavis.edu/>).

5. METLIN – Scripps Research (<https://metlin.scripps.edu>).
6. Protein – NCBI (<https://www.ncbi.nlm.nih.gov/protein>).

## 2.7 Microscopy Equipment

1. High-performance dissection stereomicroscope (e.g., Leica MZ 7.5 with 7.9:1 zoom; Leica Microsystems Inc.).
2. Transmission light microscopy inverted microscope equipped (e.g., Axiovert 25 with AxioCam MRc camera; ZEISS Microscopy).
3. UV fluorescence microscopy upright microscope (e.g., Zeiss Axio Imager.M2 (<https://www.micro-shop.zeiss.com/en/se/system/axio+imager+2-axio+imager.m2-upright+microscopes/10215/#variants>) equipped with an AxioCam 503 mono; ZEISS Microscopy, cat. no. 4109664265591000).
4. Color microscope camera (e.g., AxioCam ICc 5; ZEISS Microscopy, cat. no. 4265540000000000).
5. Fluorescence illumination system (e.g., X-Cite 120Q Iris FL Light Source; Lumen Dynamics).
6. Illuminator (e.g., VIS-LED; ZEISS Microscopy, cat. no. 4230539030000000).
7. Filter set (e.g., FL Filter Set 49 DAPI, EX G365 S free; ZEISS Microscopy, cat. no. 4880499901000000).
8. UV transmitting objective (e.g., Plan-Apochromat 10×/0.45 WD = 2.0 M27; ZEISS Microscopy, cat. no. 4206409900000000, or EC Plan-Neofluar 5×/0.16 M27; ZEISS Microscopy, cat. no. 420330-9901-000).
9. Scanning stage (e.g., 130 × 85 piezo STEP (D); ZEISS Microscopy, cat. no. 4320229902000000).
10. An image acquisition and processing package (e.g., ZEN software ver. 3.1 (blue edition); ZEISS Microscopy).
11. An image processing package (e.g., Fiji, <https://imagej.net/Fiji>).
12. Microsoft Office package for data visualization and .txt file editing (<https://www.microsoft.com/en-us/microsoft-365>).

---

## 3 Methods

### 3.1 Reagent Preparation

1. Modified Gey's balanced salt solution (mGBSS) containing (in mM) 1.5 CaCl<sub>2</sub>, 4.9 KCl, 0.2 KH<sub>2</sub>PO<sub>4</sub>, 11 MgCl<sub>2</sub>, 0.3 MgSO<sub>4</sub>, 138 NaCl, 27.7 NaHCO<sub>3</sub>, 0.8 Na<sub>2</sub>HPO<sub>4</sub>, 25 HEPES and 10 glucose, pH 7.2.
2. Glycerol stabilization solution containing 33% (vol/vol) glycerol mixed with 67% mGBSS.

3. MALDI matrix solution containing DHB saturated in a 1:1 mixture of ACN: 0.1% (vol/vol) aqueous/TFA acid. Many additional MALDI matrices are available for investigation of small metabolites, peptides, proteins, nucleotides, and polysaccharides, and can be used in biochemical profiling of single cells.

### **3.2 MALDI Mass Spectrometry Calibration**

Mass spectrometers should be tuned and calibrated before running high-throughput single cell analysis. Calibration of mass spectrometers, preferably, should be performed for each sample (e.g., ITO glass slide).

1. Time-of-flight (TOF)-TOF instruments: standards are placed on the same surface where samples are deposited. Even slight difference in distance between sample surface and mass spectrometer detector leads to variable measurements.
2. FTICR instruments (e.g., Bruker solariX): can be calibrated with secondary ESI ion source providing better options for calibration than MALDI ion source. Calibrants should cover the entire  $m/z$  range under analysis. Typically, for detection in positive mode, ion signals of peptide standards ( $m/z$  700–6000) and ion signals of MALDI matrix ( $m/z$  100–600) are used for instrument calibration.
3. Ion trap instruments (including FT mass spectrometers equipped with ESI and MALDI ion sources): can be calibrated via ESI source using commercially available ESI tuning mixes, or volatile salts of metals (such as sodium or lithium formate).

### **3.3 Solutions for Human Pancreatic Islet Dissociation and Cell Labeling**

Fresh trypsin LE islet dissociation media should be prepared as follows:

1. Prepare DPBS Tris-EDTA buffer: according to manufacturer's instructions, dilute 10× DPBS (no calcium, no magnesium) stock with Tris-EDTA buffer solution according to manufacturer's instructions, containing 10 mM Tris-HCl, 1 mM disodium EDTA, pH 8.0.
2. Prepare 10 mM stock solution of N-acetyl-L-cysteine (NAC) in 1× DPBS. N-Acetyl-L-cysteine is a cytoprotective agent against reactive oxygen species.
3. Add NAC into 1× DPBS Tris-EDTA buffer (1:100).
4. Dilute (1:1000) Hoechst 33342 of commercial stock (1 mg/mL) with 1× DPBS Tris-EDTA buffer NAC solution.
5. Dilute (1:10) 10× trypsin LE media with 1× DPBS Tris-EDTA buffer NAC solution. Antibiotics can be added to this solution as well to prevent bacterial growth during incubations.

### **3.4 Solutions for Rat Pancreatic Islet Dissociation and Cell Labeling**

1. One hour before the procedure is started, prepare 10 mL (per rat) of 1.4 mg mL<sup>-1</sup> collagenase P solution dissolved in mGBSS. 5 mM d-glucose and 0.05%–1% (w/v) bovine serum albumin (BSA) can be added to collagenase P solution [40].
2. Prepare 5 mL (per rat) of the glycerol stabilization solution.
3. Dilute (1:1000) Hoechst 33342 commercial stock (1 mg/mL) with the glycerol stabilization solution. Keep solution at 15 °C.

### **3.5 Solution Preparation**

1. Ammonium acetate sample rinsing media used after cell stabilization with glycerol: dissolve 150 mM ammonium acetate (NH<sub>4</sub>Ac) in water [41].
2. Bovine serum albumin (BSA) solution used to coat surfaces coming in touch with cells during sample preparation: dissolve 1% bovine serum in milliQ water. Can be prepared and stored at 4 °C for 1–2 weeks.

### **3.6 ITO Glass Slide Preparation**

1. Timing 2–5 min per slide.
2. Use multimeter to check the conductivity of the ITO glass surface to verify the choice of glass side and orientation of conductive surface, which is not obvious due to transparency. Note that the use of conductive glass slides is critical for analysis with TOF mass analyzers. Measurements via ion trap mass analyzers such as FTICR systems are less reliant on substrate conductivity, which allows the use of conventional microscope glass slides for sample deposition and ultimately lowers the sample preparation cost.
3. Use a diamond scribe or laser etcher to etch 1–3-mm-wide fiducial marks (can be crosses or digits), important sample information, and markups for positioning of standards and MALDI matrix blanks on conductive side of the slide. It is important to place markups on the same surface as the samples and take care in not damaging conductive surface in a way (e.g., complete circles) that would cause some regions of the slide to lose electric conductivity with other regions.
4. Wipe slides with Kimwipes, or use clean compressed nitrogen gas stream, to remove glass dust and small shards resulting from the markup process or from formation of stress cracks on the slide during etching.
5. Store slides in properly marked containers, e.g., microscopy glass storage boxes, protecting them from dust. Inscribed or etched slides can be stored at ambient conditions indefinitely.

!CAUTION Ensuring the glass slide surface is free from chemical contamination should be verified using a randomly chosen slide from the manufacturer's box before working on sample preparation. Additional washing steps can be implemented for removal of possible contamination.

!CAUTION Wear gloves and work on a clean, dust-free surface to avoid ITO slide contamination and fingerprints.

!CAUTION Scribing and etching leads to a decrease in glass slide mechanical stability – handle finished slides with care.

### **3.7 Optical Microscopy**

Optical microscopy is an important part of the described procedure. Two different systems can be used – a microscope (either inverted or upright) or histology/pathology slide scanners. These instruments should be spatially and optically calibrated/tested. Evaluation of a control/reference sample using a stage micrometer (e.g., Thorlabs part no. R1L3S1P) and fluorescent microscope slides (FSK1–FSK6) is critical for reliable and reproducible measurements. Finally, the entire workflow should be tested and optimized before starting the experiment. Here is a brief description of an Axio Imager.M2 microscope setup established using the ZEN software.

1. Turn fluorescent and transmission light sources ON.
2. Set 100% light after filter cube is going to camera.
3. Select None or DIC filter for brightfield imaging, and DAPI filter for fluorescence imaging.
4. Program sequential acquisitions of brightfield and fluorescence images.
5. Find optimal illumination for both channels.
6. Update method, saving experimentally determined settings.
7. Set acquisition of Tiled images using mosaic mode. The number of tiles, their positions, and overlap are determined at this step using the Advanced Setup option.
8. Due to the typically wide areas of samples analyzed, semiautomatic adjustment of focus should be done along the slide. Therefore, establish a set of reference points across the entire sample where the optical focus is automatically adjusted. Typically, we use 9–12 evenly distributed Focus Surface areas for automatic Z-position adjustment. It is important to determine which channel – brightfield or fluorescent – provides better options for surface focusing. Depending on the objective, magnification, and specimen, different outcomes can be achieved.
9. Under visual control, adjust and save Z-positions at each reference point.
10. Due to the large size of resulting image files (2–8 GB per tiled image), preplan and establish your image storage, processing, and export pipeline. Creating an easy-to-navigate directory structure and file naming system will save time by limiting the number of times images should be loaded for evaluation.

11. Incorporate tile stitching into the pipeline to reduce file sizes and increase the precision of cell coordinate finding.
12. Correct image brightness, contrast, and in some cases, color. This correction preferably should be done before image export into the microMS-compatible bigTIFF format. For example, due to differences in brightness of stained nuclei, increase the brightness and contrast for the fluorescent channel to levels that allow capture of the maximal number of cells, which is critical despite potential loss or distortion of morphological information. Finding of all cell coordinates is a paramount goal of this procedure. Missing low-intensity stained cells will lead to their exclusion from the distance filtering process and possible signal acquisition from more than single cell.
13. Save the method for saving tiled, stitched, and optimized images into the bigTIFF format.
14. Test method performance using small-size images.  
!CAUTION Resulting images should have minimal distortions in background to avoid formation of artifacts during image acquisition. The addition of a shading correction step at this point is important for tiled images to reduce the influence of optical path artifacts onto the final image, which may interfere with determination of localization of targeted structures or introduce faux structures.

**3.8 Optical and Mass Spectrometric Quality Control of Experimental Solutions and Supplies**

1. Use 20× objective and inverted microscope in fluorescent and transmission light modes to check for the presence of particles, including microbes and fungi, in solutions and on experimental surfaces. Dust particles may produce fluorescent signals similar to those from biological structures. Microorganism-related compounds can be detected by MS and assigned as being from sample cells.
2. If particulate matter is found in solutions, reagents, and/or supplies, filter or replace them and incorporate additional cleanup steps to ensure working surfaces remain dust- and contaminant-free (wet wiping, blowing with pressurized gas).
3. Run quality control experiments with all supplies and solutions for sample preparation as well as analyze reagents relevant to MS measurements. Create a library of signals detected. Contaminants, such as polyethylene glycols, are present in many scientific materials and reagents, and should be controlled for.

**3.9 MALDI Matrix Application**

MALDI matrix should be applied using optimal conditions for analyte extraction from the sample and mixing of analytes with MALDI matrix at the most effective ratio for the analyte class under investigation [42]. An excess or deficit of matrix can lead to poor analyte ionization, lower sensitivity of detection, and/or high



noise in the spectra. Matrix type, solvent composition, duration of contact between the MALDI matrix solution and sample, and rate of matrix drying affect matrix crystal formation, which in turn influences signal quality during measurements. The choice of MALDI matrix, as well as its solvents and additives, is critical for detection of a particular class of analytes. For recommendations, search the literature (e.g., a search of <https://www.sigmaaldrich.com> for “MALDI matrix” produced 112 entries) or instrument vendor guidelines. There are several methods for applying MALDI matrix.

1. Aerospray option 1: manual wet application using an airbrush. Multiple parameters can be adjusted for deposition of MALDI matrix onto a sample using an airbrush, including distance between airbrush nozzle and sample, spraying time, concentration of MALDI matrix, ratio of organic and aqueous solvents in this mixture, nebulizing gas flow rate, as well as physicochemical properties of solvents, e.g., volatility. Additionally, the airbrush needle/nozzle size plays a critical role in the formation of droplets of different dimensions and, respectively, different drying times. Artistic airbrushes with 0.1–0.2 mm diameter needle sizes produce the finest mist for application of MALDI matrix solution; 0.3–0.35 mm needles generate predominantly medium-sized droplets. Airbrushes with 0.4–0.5 mm needles are good for quicker application of large volumes of matrix solution.
2. Aerospray option 2: automated wet application using a commercial device. The HTX-M5 sprayer is an advantageous tool for uniform application of MALDI matrix solution onto several ITO glass slides. As an example, effective matrix deposition can be achieved with 30 mg/ml DHB in 1:1 (v:v) methanol/0.01% TFA in water applied in two passes from a nozzle positioned at a distance of 6 cm from the sample, with a nozzle velocity of 1300 mm/min, temperature of 70 °C, MALDI matrix flow rate of 100 uL/min, and matrix track spacing of 2.5 mm.
3. Sublimation (dry application): One of the best approaches for dry, thin, and relatively uniform MALDI matrix application is via sublimation [43]. This approach has demonstrated excellent performance in lipid and metabolite analysis where analytes are located on sample surfaces, e.g., on a cellular cytoplasmic membrane. However, intracellular compounds are best extracted from cells by organic solvents and internalized within the MALDI matrix crystals. The matrix sublimation/recrystallization approach was developed to enhance detectability of larger molecules, such as peptides and proteins in an  $m/z$  range of 1000–18,000 [44]. To determine the deposited matrix amount and surface density of the MALDI matrix,

ITO glass slides are weighed on a micro- or ultra-microbalance before and after the sublimation process. For sublimation, 200–500 mg of MALDI matrix is evenly distributed on aluminum foil placed at the bottom of the sublimation chamber; an ITO glass slide with mounted samples is affixed to a cold finger using double-sided copper tape. The assembled apparatus is placed in a heating mantle, medium vacuum (~10 mTorr) is developed inside, the cold finger is filled with iced water (~4 °C), and the entire system is acclimated for 5 min. The mantle is then heated 5–10 min to achieve the targeted thickness of MALDI matrix coating. Sublimation is stopped by removal of the heat source and slow venting of the apparatus, its disassembly, and sample removal.

4. MALDI matrix application approaches can be compared [45] and parameters should be optimized, depending on the results of preliminary measurements involving several differently treated samples.

!CAUTION MALDI matrix application steps should be performed in a well-ventilated space, such as a chemical hood, to avoid inhalation of MALDI matrix and solvent vapors and aerosols, which may have hazardous properties.

### **3.10 Vacuum-Assisted Liquid Aspiration Setup**

1. Liquid aspiration system built in accordance with Biosafety Level 2 regulations [46].
2. The system is connected in a chain using appropriate diameter clear, flexible plastic tubing and two 50 mL heavy wall glass filtering flasks.
3. One end of the chain is attached by the tubing to an in-house vacuum system, followed by the filter, overflow flask with punched rubber stopper with glass or plastic tube inserted, aspiration flask with punched rubber stopper with glass or plastic tube inserted, and ending with tubing of appropriate length capped with a 200 µL universal plastic pipet tip.
4. Fill 10% of both flask volumes with disinfectant liquid, e.g., freshly prepared 10% bleach solution or different chaotropic agents.

!CAUTION Filters should be replaced at least annually.

!CAUTION Disinfectant solution should be replaced after each daily experimental session.

!CAUTION Depending on the appropriate biological safety regulations, the entire system, except the filter, can be autoclaved or exposed to disinfectant according to regulations for the particular hazard and disinfection approach required.

### **3.11 Mass Spectrometer Setup**

1. Determine the laser footprint area and its position during instrument training. The laser footprint position may shift over time due to different events, including ion source cleaning

on TOF-TOF instruments. Therefore, load an ITO glass slide coated with a thin but visible layer of MALDI matrix. Completely ablate several individual spots of MALDI matrix layer with the laser.

2. Measure spot sizes and determine the morphological parameters of the laser's footprint. Note the laser footprint position in relation to the software-generated crosshair used in sample navigation, visible on the computer monitor. If laser alignment is not possible moving forward, the experimentally determined laser position should be marked on the monitor and used in instrument training.
3. Choose a method for biological data acquisition using the mass spectrometer. Manufacturer-provided default methods can be used as the starting point for sample- and analyte-specific method development. High-throughput single cell MS analysis utilizing microMS can be performed on majority of mass spectrometers equipped with sufficiently precise programmable sample or microprobe positioning. For example, we utilized two Bruker instruments [33, 38]: (1) an ultrafleXtreme mass spectrometer, set at a  $m/z$  window of 400–3000. The “Ultra” (~100  $\mu\text{m}$  footprint) laser setting was used with 300 laser shots at 1000 Hz to generate a MALDI-time-of-flight mass spectrum of each cell; (2) a 7 T solariX FTICR mass spectrometer, operated with a  $m/z$  window of 150–3000; 300 scans were collected with a 4-Mega Word time domain. Each mass spectrum was acquired with 20 laser shots at 1000 Hz and 60% laser energy.
4. Using prespotted analyte standards, calibrate the mass spectrometer.
5. Optimize the chosen method. The most useful customizations include adjustment of the laser intensity, laser footprint size and geometry, number of laser shots per acquisition, detector's gain (should be adjusted with care to ensure a longer detector lifespan),  $m/z$  range, time of delay of ion extraction (for TOF instruments), detection polarity, as well as ion optics voltages. Preparation of high-density cell population samples for realistic tuning of instrument parameters is optimal. Comparative analysis of the parameters of several default methods followed by optimization of the best-performing one may produce faster results.

**!CAUTION** To avoid mass spectrometer damage or a reduction in operational longevity, most mass spectrometer parameters should be adjusted only by specifically trained personnel or by the instrument vendor. Most MS instrument vendors provide remote diagnostics and assistance, which is a suitable for method optimization, if needed.

### 3.12 *microMS* Software Installation and Execution

*microMS* can be installed on either Windows or Linux computers, as follows:

#### 3.12.1 *Install microMS* *on a Windows Computer*

1. For the base components of *microMS* to run properly, the following software dependencies should be downloaded and installed, with links provided at <http://neuroproteomics.scs.illinois.edu/microMS.htm>: PyQt5, NumPy, SciPy, Matplotlib, Skimage, PySerial, OpenSlide, and OpenSlide Python. Most dependencies of *microMS* are included in standard distribution packages of Python 3. We have had success using *anaconda*, which also includes an IDE (<https://www.continuum.io/downloads>.) A Python 3.X (X > = 5) version must also be installed.
2. After download, PySerial and OpenSlide require separate installations. PySerial is installed by opening Windows PowerShell and entering `pip install pyserial`. This should automatically install the most recent version.
3. OpenSlide requires additional binaries, located at <http://openslide.org/download/> under Windows Binaries. Download and extract the folders, placing them in your Documents or Program files directories. The contained bin folder also must be added to the operating system path (e.g., C:\Program Files\OpenSlide\bin); see <http://www.howtogeek.com/118594/how-to-edit-your-system-path-for-easy-command-line-access/>). Once added correctly, the OpenSlide Python wrapper is simply installed by entering `pip install openslide-python` in PowerShell.
4. With the dependencies installed, *microMS* is installed by downloading from <http://neuroproteomics.scs.illinois.edu/microMS.htm> and extracting the ZIP file into a designated directory (extracted size is ~560 MB). After downloading all packages and unzipping the archive, no further installation of *microMS* is required. The main script is run with Python `microMS.py` in a command prompt in the script directory or by double-clicking the *microMS.bat* file, which runs the above command and waits for a key press.
5. To run the program, double click “*microMS.exe*”; two windows will be opened (Fig. 1).

#### 3.12.2 *microMS* *Installation and Execution* *on Linux Computers*

1. With an installation of Python 3, the required packages are installed in the terminal with `pip3 install <package>`.
2. OpenSlide is installed with `apt-get install python-openslide pip3 install openslide-python`.
3. After unzipping the *microMS* file, the main method is run with either Python `microMS.py` or `./microMS.py` after executable

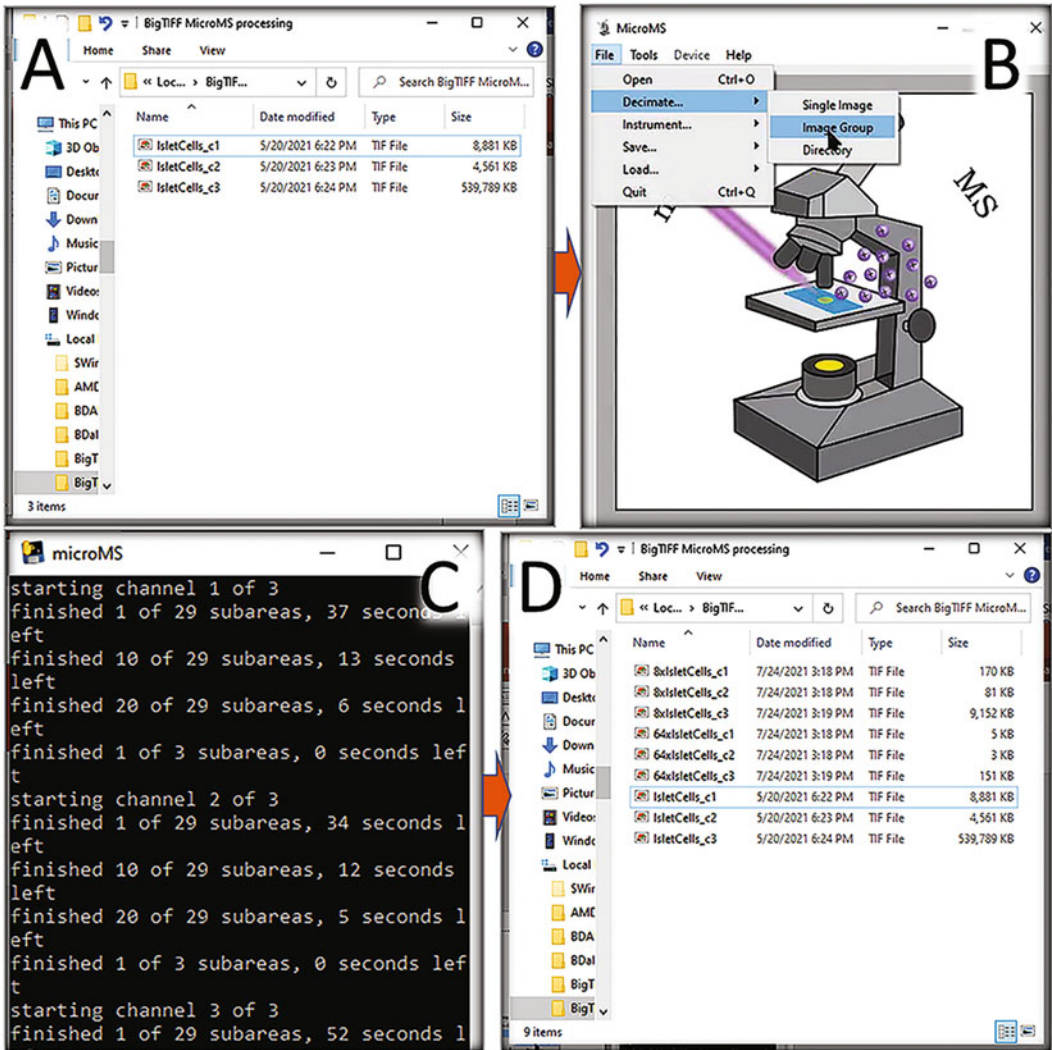


**Fig. 1** BigTIFF images may be decimated to 8 $\times$  and 64 $\times$ , generating the file sets: “8 $\times$  <image name>” and “64 $\times$  <image name>,” with <image name> being the name of original file (see Fig. 2). (a) Original bigTIFF files with names ending with optical channel abbreviations c1–c3 stored in a single directory. (b) Activation of bigTIFF decimation option for multichannel image processing. (c). bigTIFF decimation process visualized in second microMS window. (d) Original bigTIFF and decimated files

permission is granted (i.e., `chmod +x microMS.py`). Adding the microMS directory to the PATH variable will allow execution from any directory.

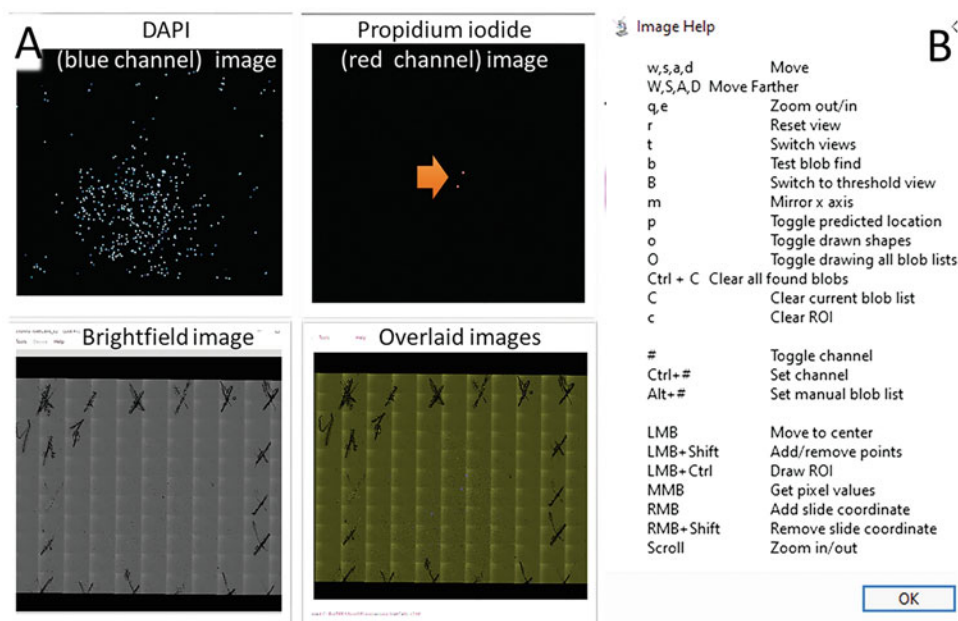


**Fig. 2** Optical image processing and operations in microMS. A population of individual cells obtained from a single human pancreatic islet is examined. **(a)** Examples of optical image views available through the “switching image channels” option. The display of different image channels is controlled through the numeric keys and is cycled with the T or Z keys. Orange arrow points toward two cell-like structures exhibiting propidium iodide staining, indicative of cell damage. Such features are excluded from MALDI MS analysis. **(b)** Image help menu describing multiple options available for image processing

## 4 Procedures

### 4.1 Islet

#### **Dissociation: Human Single Cell Populations**

Here we describe the steps required for single islet enzymatic treatment, dissociation, and deposition of populations of individual cells onto ITO glass slides.

1. Under stereomicroscope, manually collect 10–20 isolated human islets located in transportation media.
2. Transfer islets into a BSA-treated Petri dish filled with 4 mL of 1× DPBS Tris-EDTA buffer NAC solution and incubate for 10 min at 37 °C.
3. Transfer multiple islets into 1.5 mL tube filled with trypsin LE in 1× DPBS Tris-EDTA buffer NAC solution.
4. Incubate islets for 12 to 24 min at 37 °C.
5. Move all islets into a Petri dish coated with BSA and filled with ice-cold 1× DPBS Tris-EDTA buffer NAC solution. Keep dish on ice.

6. Move an individual islet into BSA-treated or low protein binding PCR tube filled with 50  $\mu\text{L}$  of  $1\times$  DPBS Tris-EDTA buffer NAC solution.
7. Mechanically dissociate islet in a tube using a BSA-treated cut pipet tip attached to a 200  $\mu\text{L}$  pipettor set to 50  $\mu\text{L}$ .
8. Deposit three 500  $\mu\text{L}$  droplets of  $1\times$  DPBS Tris-EDTA buffer NAC solution onto a new marked ITO glass slide. Make sure that the droplets remain separate.
9. Transfer solution with a cellular population formed during pancreatic islet dissociation into one of  $1\times$  DPBS Tris-EDTA buffer NAC solution droplets and agitate solution using careful pipettor-generated liquid motions. This is needed for more even distribution of cells on the ITO glass surface occupied by the droplet.
10. Wait for 15–20 min for cells to sediment and stick to the ITO glass slide's surface. Visual control under a microscope using a  $10\times$  objective is instrumental for determination of the best cell density and timing for the next step.
11. Fill a Pasteur pipet with  $\sim 1000$   $\mu\text{L}$  of the glycerol stabilization solution.
12. Replace surrounding cells  $1\times$  DPBS Tris EDTA buffer NAC solution with the glycerol stabilization solution by placing the inlet of vacuum suction system at one side of  $1\times$  DPBS Tris-EDTA buffer NAC solution droplet and adding the glycerol stabilization solution onto another side.
13. Continue to use vacuum suction system to remove the glycerol stabilization solution from the spot. Most of the solution should be efficiently removed and glycerol-stabilized cells stuck to the surface. Visible reduction in cell size can be observed due to the hyperosmotic nature of the glycerol stabilization solution. However, test measurements did not reveal the presence of endogenous peptides or lipids in the glycerol stabilization solution collected during this process. Additionally, no loss of fluorescent staining is observed. Different concentrations of up to 40% glycerol w/v are used in mammalian cell cryopreservation [47].
14. At this point, samples can be stored at 4  $^{\circ}\text{C}$  for several days, preferably in a low oxygen environment. Other storage approaches and durations should be tested experimentally for their effects on cell integrity and biochemical profiles.
15. Remove samples from storage and acclimate them to ambient conditions prior to optical imaging.
16. In most cases, some excess glycerol solution surrounding the cells remains. Glycerol solution works as stabilizer but may interfere with MALDI matrix deposition and crystallization

processes as well as influence the results of brightfield optical imaging. Therefore, remove this solution using one or two 15-s rinses with an appropriate solution, e.g., 150 mM ammonium acetate in water [41]. Remove liquid excess with a stream of nitrogen gas after each rinse. This improves the quality of extracellular solution removal.

17. If needed, add aliquots of analyte standards mixed with MALDI matrix solution onto marked spots on the ITO glass slide. These spots are important for the mass spectrometer calibration and batch mass spectra reprocessing conducted and described in Subheading 3.2.

#### **4.2 Islet Isolation and Dissociation: Rat Single Cell Populations**

Rodent islet isolation is broadly covered in the literature [40, 48, 49]. The following is a brief description of the procedure used in sample preparation for the outcomes described in Subheading 5, Anticipated Results:

1. Fill syringe with 5 mL (of the 10 mL) prepared solution containing collagenase P, BSA, and d-glucose. Preserve the remaining 5 mL of the solution.
2. Use a guillotine to decapitate Sprague-Dawley rats.
3. Surgically open the abdominal cavity.
4. Apply a clamp at the point where the common bile duct merges with the intestine, thus blocking liquid flow. Improper clamping will lead to incomplete fill of the pancreas with the digestion collagenase *P* solution.
5. Inject the pancreas with the collagenase *P* solution at the common bile duct  $\gamma$  junction, located between the liver lobes.
6. Dissect the pancreas and place into plastic tube with remaining 5 mL collagenase *P* solution.
7. Incubate the pancreatic tissues in a recirculating water bath for 20–30 min at 37 °C. A visually homogenous yellowish suspension should be formed. Taking several aliquots of suspension during this treatment for examination under microscope is helpful for determining the optimal duration of tissue exposure to enzyme. Incomplete digestion will result in formation of tissue pieces containing both acinar and islet cells. Overdigestion coincides with a loss of islet integrity.
8. Shake tube gently every 10 min of the incubation period.
9. Wash resulting suspension twice with ice-cold mGBSS.
10. Centrifuge the suspension for 3 min at 300 *g*.
11. Remove and discard supernatant and resuspend pellet in 10 mL of ice-cold mGBSS.
12. Place resulting suspension into a plastic Petri dish.



13. Place dish under inverted microscope and adjust illumination to achieve islet appearing as brownish structures and acinar tissue grayish or yellowish.
14. Under visual control using an inverted microscope, in within 10–20 min, manually isolate individual pancreatic islets using a micropipet. Typically, only 20–30 pancreatic islets collected from a single animal are needed for successful preparation of 10–15 single islet cell populations for microMS-based MALDI MS analysis. If longer time is needed, DNase (3000 U/mL) should be added into the mGBSS where dissociation of pancreatic tissue is located to prevent clumping of acinar tissue pieces and islets [50].
15. Place a single islet into 20  $\mu$ L glycerol stabilization solution containing Hoechst 33342.
16. Incubate for 2 h at 15 °C.
17. Triturate individual islets into single cells onto ITO-coated glass microscopy slides creating a low-density cellular population.
18. Repeat **steps 15–18**, described in Subheading 4.1.

### **4.3 Optical Imaging of Cellular Populations**

1. Perform tiled image acquisition using a fluorescent microscope with sufficient magnification for the given cell type.
2. Each optical channel image should be preprocessed in ZEN for optimal brightness and contrast before further processing, including tile stitching and image export.
3. Images are processed using tile stitching algorithm available in ZEN.
4. Resulting files are exported using conversion to bigTIFF [51] format using ZEN software, blue edition.
5. For microMS, any optical image data processing and coordinate finding, OpenSlide-supported image file format [52, 53] is a suitable input; however, only Hamamatsu ndpi and big-TIFF images have been thoroughly tested and are accepted by default by microMS. For multichannel images, ndpi file names should end with “Brightfield” (for channel 1, brightfield) and “Triple” (for channel 2, RGB fluorescence). bigTIFF image file name prefixes should not start with “8 $\times$ ” or “64 $\times$ .” Multichannel bigTIFF image file names require the suffix “c#.tif” where “#” is a digit between 1 and 9, typically corresponding to an optical microscopy channel, e.g., brightfield at channel 1. ZEN creates a bigTIFF file for each optical channel and names resulting file with user-defined names appended by channel information, e.g., IsletCells\_c1.tif and IsletCells\_c2.tif for two channels.

#### **4.4 Sample Preparation for MALDI MS Analysis**

1. To achieve best results, immediately after image acquisition, coat ITO glass slides with cellular populations with MALDI matrix using the matrices, solvents, and matrix deposition methods that are optimal for the research goal. Due to the large variety of sampling approaches, study goals, and variability in the equipment used, an evaluation set of samples should be prepared and tested using several approaches as guided by published information.
2. For detection of peptides in single cells, apply 50 mg/mL DHB dissolved in 1:1 (v/v) LC-grade ethanol/water with 0.1% TFA using an automatic MALDI matrix sprayer.  
!CAUTION Fiducial marks should be free of a MALDI matrix layer because it may obstruct their visibility after loading into the mass spectrometer.
3. If quantitative analysis is planned, apply aliquots of a solution containing standards for targeted analytes on several marked spots of the MALDI matrix-coated ITO glass slide. The analytical standard solution may include MALDI matrix, or you can omit it if the solution solvents are capable of dissolving the deposited MALDI matrix layer. Choose standard deposition locations far from cell populations to avoid contamination. Also, the locations should be easy to find after sample loading into the mass spectrometer.
4. Generated samples can be stored at room temperature in a desiccator or N<sub>2</sub> environment for 24 h. Storage at lower temperatures, e.g., 4 °C to –80 °C, helps to preserve biological samples for different MS applications [54, 55]. It is important to experimentally determine the optimal sample storage time and conditions for each sample type. Reduction of sample exposure to oxygen and excessive moisture, e.g., due to water condensation on cold specimens, can be critical for successful measurements.

#### **4.5 Processing Optical Images with microMS: Finding Cell Coordinates and Output Filtering**

Also, see the microMS manual: <http://neuroproteomics.scs.illinois.edu/microMS.htm>, for more details.

1. Start microMS. On startup, the main GUI window is displayed with the program icon and a second window for visualization of the operational steps and errors (Fig. 1b).
2. Opening an image in microMS can be done in several ways, depending on the image type, desired spatial resolution, and procedure goal. Images that do not need to be magnified during operation, e.g., images covering small areas, can be loaded unmodified by selecting Open in the File menu (or Ctrl + O). This will launch a file selection dialog that prompts the user to select the desired file, which will subsequently be loaded. Selecting any image from a multichannel-

data image set located in the same directory will open all channels with matching filenames, as described above. Multiple image channels (if they exist) are loaded at the same time and overlaid on top of each other without image flattening. However, by default, non-pyramidal bigTIFF images can only be zoomed out by 4 $\times$ . bigTIFF images may be decimated to 8 $\times$  and 64 $\times$ , generating the sets of files “8  $\times$  <image name>” and “64  $\times$  <image name>” with <image name> being the name of original file (Fig. 1). This will enable further zoom levels from 1 $\times$  to 1/256 $\times$  (which is recommended).

- (a) bigTIFF image sets are decimated by selecting the Decimate option in the File menu. Several options are available: both “Single Image” and “Image Group” options are for the selection of one bigTIFF image. However, when a single file of a multichannel-data image set (e.g., IsletCells\_c1.tif) is selected with the “Image Group” option, all images (e.g., IsletCells\_c2.tif) of the set will be decimated. The “Directory” option allows the selection of a single directory. All images contained in sub-directories of the selected directory will be decimated.
  - (b) Notice that since a single image (brightfield) was decimated, only the specified channel is displayed at higher zoom levels. After decimation is complete, the process does not need to be repeated the next time the image set is opened. Opening the single non-decimated image file through Open in the File menu will automatically load the full image stack.
3. Use the image navigation features of microMS to visually inspect loaded and displayed images. A list of mouse and keyboard controls are available through Help > Image Hotkeys (Fig. 2). Depending on the size of the image and computer performance, response time for these operations can be different. Working with image files located on network drives or USB2-connected devices may increase this time even further.
  4. Perform previous step for all optical channels, switching between image features available in microMS. The same list of mouse and keyboard controls available through Help > Image hotkeys can be used. As an example, displaying different images for different optical channels is controlled through the numeric keys and is cycled with the T or Z keys (Fig. 2a).
  5. Determine the sample area(s) to be processed with microMS. By default, the entire optical image area is subjected to processing. However, only a portion of the ITO glass slide is occupied by cell populations. Therefore, to reduce processing time, regions of interest (ROI) can be created on the analyzed images so that finding of cell-like structures will be restricted to

selected ROI. A single rectangular or polygonal ROI can be created by holding Ctrl + left mouse button (LMB) and dragging the cursor to form a yellow rectangle around the ROI. To create polygonal ROI, a rectangular ROI should be drawn, followed by its modification by (a) holding Ctrl + Alt, (b) placing cursor nearby one of yellow side lines, (c) dragging the cursor to a desired location leading to outlining of ROI with yellow, and (d) clicking of LMB to finalize the modification. Polygonal ROIs also can be formed by holding Ctrl + Shift and consecutively clicking LMB and dragging the cursor. The ROI can be removed by pressing the “c” key.

6. All structures detected on the images via user-defined parameter settings in microMS are called blobs (cells and other structures). With optimal sample preparation, image acquisition, and microMS parameter settings, most blobs will represent individual cells. During the automatic blob finding process, each blob has the following parameters determined: an x-y coordinate, an effective radius, and the object’s circularity. To start automatic blob finding, several blob parameters, such as minimum size (in pixels), maximum size, minimum circularity (shape), maximum circularity, threshold (lower threshold for acceptable pixel signal intensity), image channel, and color, should be imputed into Blob Find Entry window opened through Tools > Blob Options (Ctrl + B).
  - (a) By default, image channel 1 corresponds to the brightfield image. The intensity thresholding is done on one of the RGB channels, allowing more specific and precise localization of the cellular features of a sample. Some of parameters can be left blank, e.g., maximum size and maximum circularity.
  - (b) Activation of added parameters is done by clicking “Set Parameters.” This will lead to automatic resizing of the current image to maximal magnification and markup of visible blobs detected according to the set parameters with green circles. This option represents a quick way to determine the efficiency of the selected parameters. Visualization of a different area of the image will lead to markup of visible blobs with characteristics according to the set parameters.

**!CAUTION** Different strategies can be used to optimize the blob finding parameters, which are critical for determination of the coordinates for most of the individual cells. However, if the parameters are too strict, they may exclude a number of sample structures from the next steps, such as distance filtering. This may lead to mass spectra acquisition from several closely located structures due to the relatively large laser beam

footprint (e.g., 100  $\mu\text{m}$ ). Therefore, it is important to obtain information on the localization of the maximum number of structures before distance filtering, followed by removal of size-incompatible features, e.g., large cell clusters or single nuclei released from damaged cells. This challenge can be addressed at the sample preparation stage when low-density populations of intact single cells are deposited on the ITO glass slide.

7. To find cell-like structures (i.e., blobs) (Fig. 3), use Tools > Blob Find to initiate finding according to set parameters. This process can take from several seconds to several minutes. At the end of the process, a window “Save All: Enter base filename” pops up. Enter desired file name to save information on found blob list in the .txt file located on the same directory where the original images are located.
8. Visually examine the detected blobs, which will be outlined by circles (Fig. 3b). For faster processing, only 150 blobs will be outlined in the field view. To mark all blobs, uncheck Tools > Limit Found Blobs. Alternatively, found blobs and other structures not selected as blobs but exhibiting above threshold signal intensities can be visualized as uniquely color-coded features on a dark blue background by pressing Shift + B, activating/deactivating threshold view. Pointing the cursor to a blob of interest and clicking on the middle mouse button will generate information on its area and circularity in the status bar. This information can be instrumental for optimization of the blob finding process.
9. Create an additional blob list if unsatisfactory blob finding occurs and if there is a need for comparison of different blob lists. Up to ten different blob lists can be saved and quickly compared. Alt + “the blob list number” will toggle different already populated or empty blob lists. Choose an empty blob list (0 blobs indicated in info line), change Blob Options, and repeat the blob finding process; a new blob list and corresponding file will be created and assigned chosen list number. This process will result in the appearance of a new set of marked blobs. Additionally, saved blob lists can be loaded through File > Load > Found Blobs. All created blob lists can be visualized using the key combination Shift + O. Overlapped blobs will be marked by circles of blended colors.
10. If needed, filter blob list using ROI filtering. A ROI can be created and blobs inside or outside of this ROI retained or removed. Tools > ROI Filter Retain and Tools > ROI Filter Remove are used in this procedure, which can be performed at any time after blob finding. The ROI Filter Retain operation removes all blobs outside of the specified ROI and moves the resulting list to the next open blob list. The ROI Filter Remove

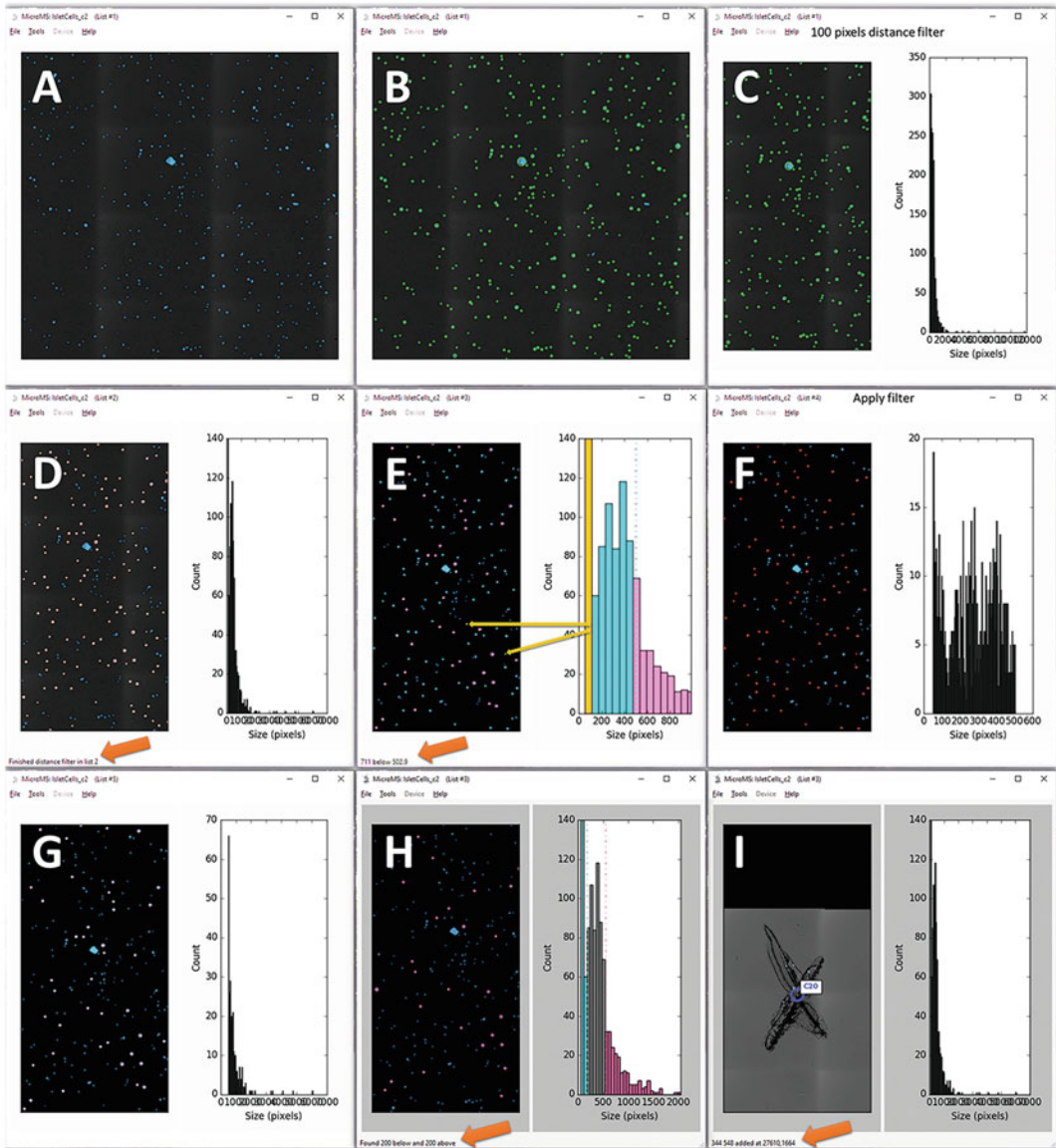


**Fig. 3** Examples of major steps in blob finding and selection as well as defining of fiducial marks. (a) Original decimated three-channel overlay image of single human pancreatic islet cellular population. (b) Results of blob finding procedure with minimal restrictions performed on blue channel image. Blobs are marked with green circles. (c) Histogram window shows size distribution for all detected blobs. (d) Results of distance filtering, cutoff at 100 pixels. Blob list #2 is automatically created. Blue and orange arrows point to related displayed information. (e) Results of blob size filtering followed by histogram markup and filtering. Results of manual single bar markup are shown in yellow. Blue bars of the histogram relate to blue circled blobs on the image. The same is true for pink bars. Yellow lines point to two blobs corresponding to selected yellow bar. Command “Apply filter” leads to formation of two new blob lists (from e): (f) list #4 for blue bars corresponding cells and (g) list #5 for pink blobs. (h) Histogram and selected blobs for “Peak extremes” option of microMS; 200 blobs above and 200 blobs below the average are found and marked. (i) Example of manually added markup of a fiducial point from the brightfield image. Images of small areas of one single cell population are demonstrated. Orange arrows point to information line appearing after different calculation steps

places all blobs outside the ROI into a new list. In both cases, the original blob list is not modified and retains its number.

11. If needed, new blobs larger than 10 pixels are added to the current blob list with a Shift + left mouse button (LMB) click. Toggling of this key sequence will mark or unmark selected blob. Shift + LMB click and dragging of cursor allows the user to mark larger blobs. It is critical to manually create blobs at ITO glass slide locations where analyte standards are deposited. Mass spectra acquired from these sample areas can be used in batch mass spectra reprocessing during the data analysis phase detailed below.
12. If needed, perform filtering of blob lists using collected (during automatic blob finding) information on blob size, circularity, pairwise distance, and average signal intensity at chosen fluorescence channel. Pairwise distance filtering is a recommended first step, which allows detection and removal of blobs that are too closely located for independent analysis by MALDI MS. This and other filtering options are realized through the histogram interface of microMS. Tools > Histogram Window (Ctrl + H) opens the graphic window (Fig. 3c, d). Shortcuts for histogram navigation and function operations can be visualized through Help > Histogram Hotkeys. The histogram will be automatically updated after each operation, e.g., by switching to another blob list or executed filtering. Tools > Histogram Options leads to a pop-up window allowing a number of parameters for filtering to be selected, including image channel, blob parameter (optical channel color or morphology: size, circularity, or distance), offset (to the amount to increase (>0) or decrease (<0) the blob radius when examining the blob region), and level of optical signal intensity within the outline of the blob. To save histogram information, use File > Save > Histogram Image (.png file is generated) and File > Save > Histogram Values (tab delineated text files containing information on x-y coordinates and corresponding metric value for each blob are saved). microMS has a number of helpful functions for visual assessment of the results of histogram-based filtering, including visualization of blobs that correspond to a particular bar of the histogram using the middle mouse button (MMB) to click on a single bar (Fig. 3e). Vice versa, a LMB click on a blob will highlight the corresponding bar. Clicking capital C as well as switching to another blob list clears all histogram information. A right mouse button (RMB) click on the histogram sets the upper threshold for the filtered blob parameter (information on number of blobs above threshold is presented and responsible blobs are color marked), and LMB sets the lower threshold (information on number of blobs below threshold is presented and

responsible blobs are color marked). For automatic finding of peak extremes in a blob population, first select a range of bars in the histogram using Shift + LMB (lower cutoff) and Shift + RMB (upper cutoff) and then select Tools > Peak Extremes (Fig. 3h). A pop-up window will allow the user to set the number of blobs that will be searched for in high and low ranges selected for the blob population.

13. In instances where several filters need to be applied for even more selective defining of a targeted blob list, visually verified filtering results should be consecutively saved as new blob lists (Ctrl + A or Tools > Apply Filter) (Fig. 3f), or as new files containing blob lists (File > Save > Histogram Divisions).
14. If needed, utilize the blob patterning feature of microMS for analysis of large structures, such as multicellular pancreatic islet aggregates or even entire islets. This option allows the user to generate nine or more acquisition points per blob. Multipoint signal acquisitions can produce better results than single-point acquisition. Due to the focus of this protocol on single cell analysis, please refer to the online microMS manual for more details on this feature.
15. Save resulting blob lists using one of the following options: (a) File > Save > Current Blobs (only current blob list is saved), (b) File > Save > Histogram Divisions (saves information on histogram filtered low- and high-intensity populations as separate files), and (c) File > Save > All Lists of Blobs (all blob lists are saved in separate files). Editable text files will be created. Loading of saved blob lists using File > Load > Found Blobs will overwrite current information, which should be saved in advance if important.

#### **4.6 High-Throughput Single Cell MALDI MS: microMS and Mass Spectrometer Information Co-registration**

1. Take sample coated with MALDI matrix from storage and, if needed, acclimate to room temperature, preferably under vacuum.
2. Load acclimated specimens into a MALDI TOF-TOF mass spectrometer.
3. Using spots with calibrants, blank areas, and a test area with cells deposited, create and optimize instrumental methods appropriate for the experimental conditions and research goals (Fig. 4).
4. To co-register the optical imaging information and the mass spectrometer coordinates, run both microMS and the mass spectrometer operating software (e.g., Bruker flexControl).
5. Ablate a single spot on the MALDI matrix-covered area of the sample to visually determine the spot's location on a video output from the mass spectrometer. Mark this position for easy finding during coordinate system alignment. The laser



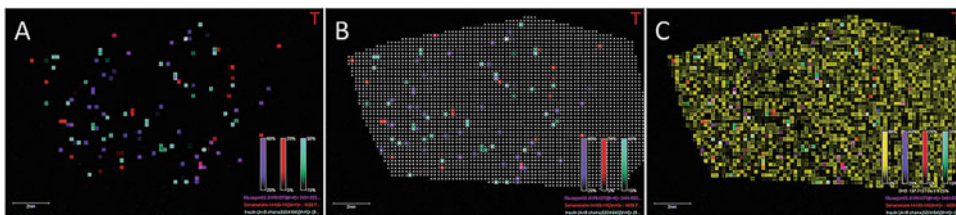


**Fig. 4** Mass spectrometry imaging-based testing of a sample area prepared for microMS-assisted analysis. Cells are from a single human pancreatic islet. **(a)** Molecular image of distributions of three major pancreatic islet hormones – glucagon (pink), somatostatin (red), and insulin (green). **(b)** The same image as in **(a)** with the positions of laser sample probe shown. **(c)** The same as in **(a)** with distribution of MALDI matrix signal (yellow) added

beam footprint position may change over time due to mechanical misalignment that may occur during regular manual ion source cleanup. Even a 50  $\mu\text{m}$  shift may lead to significant alteration of data output.

6. Load processed optical images for the sample under investigation into microMS. Only filtered blobs that have been targeted for analysis should be circled on the microMS displayed image.
7. Choose the analysis instrument in microMS by selecting File > Instrument. Several options are available by default, including the Bruker ultrafleXtreme MALDI TOF-TOF and solariX FTICR instruments.
8. Co-register the fiducial markers on the optical image displayed in microMS and the same physical markers visible on the video output from the mass spectrometer. Under visual control, align the sample plate position and the first fiducial mark on the mass spectrometer's computer monitor where the laser beam appears during acquisition. Find the same fiducial mark on the image displayed in microMS and click RMB (Fig. 3i). A pop-up window will appear asking the user to "Enter plate coordinate"; the x-y coordinates of the sample plate aligned in the mass spectrometer should be entered, e.g., 9494 3493, where the first number is the x-coordinate and the second is the y-coordinate, separated by a space. The actual sample plate coordinates can be found in several places within the instrument's software. For example, for the ultrafleXtreme, flexControl displays this information in the Sample control window. Copy and paste the displayed values into the pop-up window in microMS and click OK. A blue circle marked with the letter and number corresponding to the default plate spot numbering for a Bruker MTP glass slide II adapter will appear. Move to another fiducial mark in microMS, find the corresponding fiducial on the mass spectrometer, and repeat the process. More fiducial marks used for each ITO glass slide provides enhanced coordinate alignment. At times an individual fiducial

appears inconsistent with others; this is marked with a red circle to indicate the fiducial with the worst alignment compared to the other fiducial marks. If it appears there is an error in a specific mark, this can be deleted by pressing RMB + Shift. It is recommended to proceed to completion with the remaining fiducial marks.

9. Save the co-registration information in microMS using File > Save > Registration; a .msreg (mass spectral registration) file will be created containing information on the instrument name and fiducial set characteristics. The saved co-registration can be loaded through File > Load > Registration.
10. Save the fiducial positions using File > Save > Fiducial Positions, producing an instrument-specific .xco file with information on fiducials. This file can be loaded into a mass spectrometer to determine the accuracy of the co-registration process.
11. Save the information on found and filtered, currently displayed blob list using File > Save > Instrument Positions forming an .xco file. File is instrument-specific. During the save process, three prompts will appear. The first allows the user to specify file name and location. The second allows the user to set the maximum number of blob positions that will be saved. The third provides a choice between two options related to the order in which blobs will be analyzed with MS. microMS incorporates a simplified version of the traveling salesperson path (TSP) optimization. The TSP approach determines the minimum stage movements required to target all selected locations. Thus, choosing the TSP option significantly reduces the sample plate movement time needed for analysis of all blobs. However, there is a correlation between computer performance, number of blobs, and time needed to calculate the optimal path using the TSP algorithm. Considering that the steps of this protocol, starting with co-registration of fiducial marks, require mass spectrometer engagement, TSP calculations for very large blob lists may require more than the 3 min allocated for this operation. Therefore, finding the optimal number of blobs for such operation can be determined for your specific computer system. Splitting of large blob lists into several smaller ones by identifying ROI is one approach to reduce the sizes of blob lists without compromising the number of blobs analyzed. We have found that TSP is very useful for most measurements.
12. It is a good idea to repeat the measurement of a small portion each sample (Fig. 5). This test allows the user to determine if the MALDI matrix and spatially co-localized analytes are completely desorbed at each targeted cell. Incomplete use of

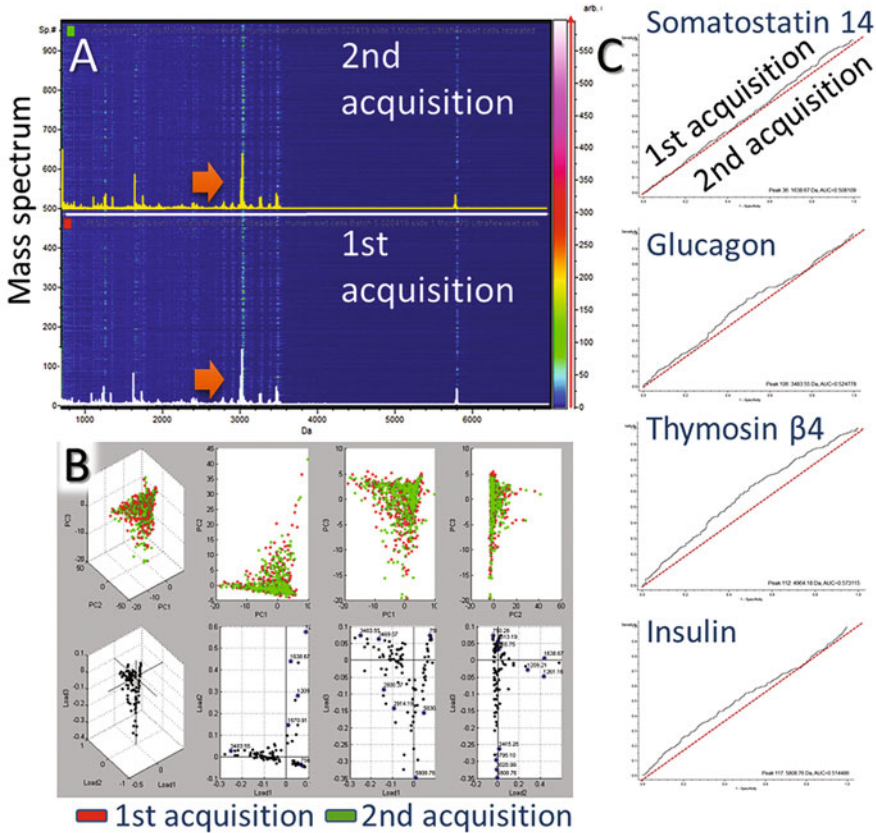


**Fig. 5** Test for completeness of MALDI matrix ablation during microMS-assisted high-throughput single cell MALDI MS analysis. The same human pancreatic islet cells were analyzed twice. (a) Gel view of mass spectra acquired twice from 498 cells. Arrows point to average mass spectra for all cells acquired during corresponding set of acquisitions. The mass spectra are overlaid with gel views. (b) Results of PCA of acquired data sets. (c) Receiver operator characteristic curves for selected analytes detected in repeated measurements of the same sample

sample/matrix in a single run suggests that one is not producing the best possible signals. However, it also creates an opportunity to reanalyze the same cells using different instrument settings, including the use of MS2-based analyte sequencing.

#### 4.7 High-Throughput Single Cell MALDI MS: Data Acquisition

Here we describe the procedures for a MALDI TOF-TOF mass spectrometer (we used the Bruker ultrafleXtreme mass spectrometer and software); similar procedures can be used for FTICR mass spectrometers (e.g., the Bruker solariX).

1. Copy microMS-generated fiducial positions and the instrument registration .xco file into Data\Methods\GeometryFiles.
2. In flexControl, load the Method intended for analysis of microMS-defined blobs.

3. Optimize acquisition parameters and calibrate the mass spectrometer using the Method and analyte standards deposited on ITO glass slides.
4. Using flexControl, create an AutoXecute Method through the Method: Edit option in the AutoXecute window. Use the calibrated and optimized method during AutoXecute Method creation. The number of laser shots per acquisition and laser intensity used for an automatic run should be specified in the AutoXecute Method. Importantly, if batch reprocessing of acquired mass spectra are planned for the data analysis stage (discussed below), also include and specify standard calibration spots and flexAnalysis methods. These parameters are defined during the Run Editor operation described in the following steps.
5. Create a new run by selecting Run: New option in AutoXecute window. The AutoXecute Run Editor window will pop up. Choose File > New Run Wizard (Ctrl + Shift + N) to open the New Run: Target geometry page. Mark Start with wizard at this page. Find and mark the .xeo file. Hit Next; the laser power tuning page will appear. Follow instructions on the page and click Next. Calibration and sample spot selection page will appear. Follow instructions by pointing, holding, and dragging cursor from top left to bottom right corner of empty space on the right side of the window. This will select all microMS-determined blobs listed in the .xeo file. Hit Next. The Run Parameter page will appear where the AutoXecute Method, Data Destination: Data Directory, and Sample Name should be specified. Keep lengths of both to a reasonable minimum if peak list export into Excel spreadsheets is planned (described below in Data Analysis and Processing sections). More options are listed and can be used during the AutoXecute run. Importantly, flexAnalysis MS and MS/MS methods should be included in the AutoXecute run at this point to allow some types of future batch mass spectra reprocessing, if needed. (Consult the flexControl manual or Help for instructions.) Hit Next. A summary of the New Run Finish page will appear. Click Finish. This will close the New Run Wizard.
6. In the remaining open AutoXecute Run Editor, click, hold, and drag cursor, starting from upper left corner of unmarked empty space located on the left upper side of the window. Releasing the cursor at the right bottom corner will again mark all microMS-determined blobs, which were invisible before this selection step. Hitting OK opens the prompt for naming and saving the AutoXSequence file. Saving the file results in closure of the AutoXecute Run Editor and opens the window for

Messages. This usually informs the user about Factory teaching points; these cannot be loaded in case of custom teaching done through co-registration of image file in microMS and the video output of mass spectrometer. The Messages window can be closed.

7. Hit Start Automatic Run in the AutoXecute window. Automatic acquisition of data from all specified blobs will start. As a result, the data directory specified during the New Run Wizard procedures will be populated with folders containing individual mass spectra.

#### **4.8 Data Processing and Analysis Using ClinProTools**

ClinProTools is a user-friendly program with an integrated set of tools for biomarker discovery and clinical proteomics search. It supports MS data post-processing and statistical profiling workflow to detect biomarker patterns indicative of specific cell types. We find the program help files and user manual informative regarding the available analysis functions and guidelines on the choice of statistics. Included below is an example of a workflow for a two-group experimental comparison.

**!CAUTION** Mass accuracy of MS measurements depends on many factors [56–58]. Therefore, before analysis of each data set, determine if recalibration of the mass spectra is needed. The entire data set or just representative mass spectra should be loaded into ClinProTools (or flexAnalysis as described in the following section) and precision and accuracy of measurements determined. Both programs allow mass spectrum recalibration.

1. Split the entire data set into several new folders according to the desired comparison traits. For example, we split 485 mass spectra acquired from one pancreatic islet population into two folders.
2. Set ClinProTools Data Preparation > Settings Spectra Preparation parameters.
3. Set Data Preparation > Settings Peak Calculation parameters.
4. Sequentially load two sets of mass spectra from the two different folders into ClinProTools.
5. Using File > Save Class Paths, create an XLM file with information on the location of all individual mass spectra loaded for analysis.
6. Run Statistical Analysis > PCA. Confirm Scaling Method: Level. New window with Score plots and Loading plots will appear, and automatically selected peaks will be marked in the mass spectra window. There are two main outputs of the analysis. One is related to finding of characteristic profiles for

different mass spectral groups corresponding to different cellular populations. Loading plots allow the user to determine specific signals that contribute to profile differences among cellular phenotypes. The other is the ability to export calculated information on signal parameters into a table format, as described below.

7. Save results in an Excel-compatible XML3 format using File > Peak List Export option. This option also allows the user to export information on all selected peaks in several other formats. The XML3 format provides information on the class and spectra paths as well as peak area and intensity as two separate tables. Importantly, ClinProTools generates information on intensity and area for all mass spectra, including ones that have no peaks in the automatically selected  $m/z$  region. As a result, the generated tables have no missing values, which are typical for many types of mass spectrometric measurement outputs. This allows straightforward statistical analysis, including sorting of mass spectra lists by biomarker information and reloading of mass spectra sorted by groups into ClinProTools for more detailed statistical analyses.
8. To open the XML3 file in Excel, a style sheet reference for ClinProtPeakList.xsl should be found in C:\BDAL\ClinProTools\_3\_0\Files and copied to the same directory where the XML3 file with results is located. When opening the file, a pop-up with warning message about file format and extension will appear and should be ignored by clicking “Yes.”
9. In most cases, signal intensity is one of the most common parameters in the statistical analysis of MALDI MS-acquired data. Therefore, choose Intensity table and perform data sorting according to chosen biomarkers.
10. Evaluate individual mass spectra to determine the minimal signal intensity for a particular biomarker and split the table into two sections. Perform data sorting for another biomarker in the remaining data set and repeat the steps above. As a result, the entire data set will be divided into a number of classes according to signal intensities of the chosen biomarkers.
11. Using the Excel CONCATENATE function, transform the resulting table into a single column table with information structured as follows:

```

<ClinProtSpectralImport Version="0.0">
  <Class Name="Class A">
    <Element Path="C:\A\0_M16_1SLin\fid"/>
    <Element Path="C:\A\0_M17_1SLin\fid"/>
    <Element Path="C:\A\0_M18_1SLin\fid"/>
  </Class>
  <Class Name="Class B">
    <Element Path="C:\B\0_M19_1SLin\fid"/>
    <Element Path="C:\B\0_M20_1SLin\fid"/>
  </Class>
</ClinProtSpectralImport>

```

where “Class A” can be replaced with custom name for the data class and information on data path, e.g., “Y:\microMS\Islet cells\1\0\_x\_17134y\_16568\1\1SRef” enclosed in parenthesis.

12. Save resulting table in Extensible Markup Language (XML) file using Excel. Alternatively, the single column table can be copied into the free software Notepad++ (<https://notepad-plus-plus.org/>) for additional checking, formatting, and then saving as an XML file.
13. Open newly created XML file in ClinProTools through File > Open Spectral Import XML.
14. Perform new set of calculations, including PCA, pLSA, and unsupervised clustering.
15. Export results through Reports option.

#### **4.9 Data Processing and Analysis Using flexAnalysis**

One drawback of using ClinProTools for a large number of mass spectra is the need for significant data reduction, e.g., by a factor of 30–50. This leads to a noticeable reduction in mass resolution and the accuracy of  $m/z$  values determined for each of detected compounds. Therefore, complementary analysis of data sets can be performed in flexAnalysis.

1. Open flexAnalysis and load representative mass spectra for all predetermined classes.
2. Load mass spectra of analyte standards acquired during the same set of measurements.

3. Determine if mass spectra require recalibration. Sometimes mass spectra acquired at different ITO slide locations require recalibration, which can be done manually in flexAnalysis. Unfortunately, no batch recalibration option is available unless calibration mass spectra are included in the AutoXecute run sequence.
4. Using Method > Edit Processing Method (Active Settings), optimize Mass list and Processing parameters or use default settings.
5. Perform Mass List > Find operation resulting in peak finding, markup, and population of Mass List window with selected set of parameters. A variety of individual signal parameters can be chosen, including  $m/z$ , time-of-flight, signal intensity, signal-to-noise ratio, quality factor, resolution, signal area, relative intensity, full width at half maximum (FWHM), and chi-square value.
6. The Export\Mass List to Excel command creates an individual spreadsheet in a new Excel file for each reprocessed mass spectrum. Spreadsheets are automatically named with the directory name containing the mass spectrum. Due to restrictions on the length of spreadsheet names, some directory names are truncated. The process of spreadsheet creation will stop when a second identical name is generated. Therefore, it is strongly recommended to keep the length of data set names to a reasonable minimum. Additionally, with the availability of proper data converters allowing access to proprietary data formats, mass spectra generated by instruments of different vendors can be converted into general formats such as mzXML, which are readable by third-party software, e.g., MathWorks Mass Spectrometry and Bioanalytics toolbox [59, 60]. Bruker's CompassXport is one such converter.
7. Use the Process Menu > Batch process macro for reprocessing of multiple mass spectra. Mass spectra recalibration, baseline correction, smoothing, normalization, and peak picking are among the recommended reprocessing steps [61]. For large sets of mass spectra, a data reduction procedure can be implemented [62]. Mass spectra in a chosen folder, or those related to particular AutoXecute run, can be selected for reprocessing. Importantly, flexAnalysis MS and MS/MS methods should be included when creating the AutoXecute run described above. A variety of reprocessing functions can be performed in batch mode, including mass spectra smoothing, peak picking, and peak list export. flexAnalysis methods are editable through the Method > Edit Script option. Multiple processes can be included in a single flexAnalysis method.



8. Correlate ClinProTools- and flexAnalysis-generated peak lists and use the most accurate  $m/z$  values, which typically are generated by flexAnalysis.

#### 4.10 Ways to Assign the Detected Signals

Typically, single cells contain insufficient material to allow structural characterization of multiple analytes using MALDI MS/MS. Correlation to CE-ESI MS/MS or LC-ESI MS/MS data on identical tissue or bulk cell suspensions often provides more information on the chemical identity of biological constituents. However, there is often a partial overlap between ions detected by MALDI MS and ESI MS, making direct comparison of data sets less straightforward. There are several approaches available to help address this challenge. One option is a combination of single cell MALDI MS data, published information on analyte presence in cells and related tissues, and identifications from the LC-MS/MS data.

Alternatively, putative assignment of detected peptides can be based on mass match to predicted peptides from known proteins available in different databases such as UniProt [63, 64] and the NCBI Protein Database [65]. In silico peptides should be calculated not only as typical monoprotonated  $[M + H]^+$  ions but also frequently detected sodiated  $[M + Na]^+$  and potassiated  $[M + K]^+$  molecular ions typically detected by MALDI MS operating in positive polarity mode. Steps for using UniProt to create a list of putative ions for human islets of Langerhans, and NeuroPred, a useful tool for prediction of prohormone/secreted protein post-translational processing (<http://stagbeetle.animal.uiuc.edu/cgi-bin/neuropred.py>) [66], are provided below.

##### 4.10.1 Using UniProt

1. Go to <https://www.uniprot.org/> and initiate search using keywords related to annotation type and organism, e.g., annotation:(type:peptide) organism:human. (Our search resulted in 454 entries with known endogenous peptides.)
2. To visualize information and links on peptides, use the “Columns” option to add new non-default columns such as Peptide, Transit Peptide, Modified residue, Post-translational modification, and Disulfide bond.
3. Mark and copy entire area containing the search results and paste it into an Excel spreadsheet. This information can be also saved into a variety of formats (including Excel) via the “Download” option. However, links and particularly useful formatting in sub-tables will be lost.
4. Unmerge all columns in Excel and expand information on Entry, Entry Name, Gene Name, and Protein Name specific to each peptide to newly formed cells in corresponding columns.

5. Align in the same rows, information on Modified Residues and peptides that have them. New columns may need to be added because multiple modified residues are often present in the same peptide.
6. Add an additional column for peptide sequences, e.g., “Peptide Sequence,” which can be found by clicking on corresponding links in the “Position(s)” column. A new web browser BLAST window will open, presenting information on the peptide sequence.
7. Copy and paste this information into new “Peptide Sequence” column.
8. When the “Peptide Sequence” column is populated, add new column “Peptide Monoisotopic Mass.”
9. Download the NIST Mass and Fragment Calculator from <https://www.nist.gov/services-resources/software/nist-mass-and-fragment-calculator-software>.
10. Copy and paste entire “Peptide Sequence” column into Sequence window of the Calculator. Select “Monoisotopic mass of peptide sequence” and click “Formula.” A table containing the Peptide formula, its monoisotopic mass, and sequence will appear in lower window.
11. Copy and incorporate this table into the Excel spreadsheet.
12. Create a list of putative ions by adding to or subtracting from peptide monoisotopic mass values associated with PTMs specified in the table, as well as proton, sodium, and potassium adducts. Information on monoisotopic masses for these entries can be found at several locations including <https://www.uniprot.org/docs/ptmlist> and <https://fiehnlab.ucdavis.edu/staff/kind/metabolomics/ms-adduct-calculator/>. This procedure will create at least three  $m/z$  entries for each peptide. Pay attention to peptides that have two chains linked by disulfide bonds, e.g., insulin. Only separate chains are listed in the Peptide tables. Therefore, their combined monoisotopic masses should be calculated and corresponding PTM and ion-forming modifications calculated.
13. Create a combined table of putative and measured peptides. Sort all entries and find close to identical  $m/z$  values.
14. If all ions cannot be identified using UniProt, test the information on identified peptides using the peptide mass fingerprinting [66–68] approach [64, 65, 67] for protein identification. Several open-source modeling tools are available on the ProteinProspector portal <https://prospector.ucsf.edu>.

#### 4.10.2 Using NeuroPred

The basic steps are outlined below, with detailed instructions available on the NeuroPred site. There is no batch processing option in NeuroPred, and predictions can be made for individual prohormones.

1. Use the FASTA sequence format to paste the protein of interest into The Sequence Submission Box of NeuroPred (<http://stagbeetle.animal.uiuc.edu/neuropred/neuropredinput.html#sequenceformat>).
2. Fill the prediction parameters box as desired (include signal peptide length, PTMs of interest, etc.). Importantly, select a relevant animal model for your search before submitting the search. In our case, we selected the Mammalian prediction model.
3. NeuroPred will generate a list of theoretically possible peptides resulting from endogenous enzymatic prohormone processing according to known cleavage rules observed in mammals. Note that resulting list of putative processed peptides needs additional sorting upon export in Excel to remove peptides with untrimmed basic residues and products of missed cleavage (if this option was enabled during setup).
4. Combine all tables, perform additional data sorting, and perform additional search.
5. Ambiguous mass matches to predicted peptides can be validated by modeling the isotopic cluster of predicted sequence against experimentally observed peptide isotopic envelop pattern. In flexAnalysis, this can be achieved by using the Smart-Formula function.

---

## 5 Anticipated Results

microMS-supported high-throughput single cell MALDI MS provides individual profiles on populations of thousands of cells. Because of the nature of MALDI MS and the low amounts of material within a cell, only the most abundant analytes are detected, while assessment of large populations enables statistical comparisons and insights into cellular heterogeneity. For example, within the populations of individual cells from rodent pancreatic islets, peptide profiles representing the expected cell types ( $\alpha$ ,  $\beta$ ,  $\delta$ , and PP cells) containing the canonical islet peptides are detected (Fig. 6a) [32]. The approach described here allows detection of more than 300 molecular futures in the 1000–7000 molecular mass range among individual cells. With optimal sample preparation and tuning of the MALDI TOF-TOF mass spectrometer, even a single cell sample can generate mass spectra of higher molecular weight peptides at >8 kDa with a mass resolution and accuracy from sub

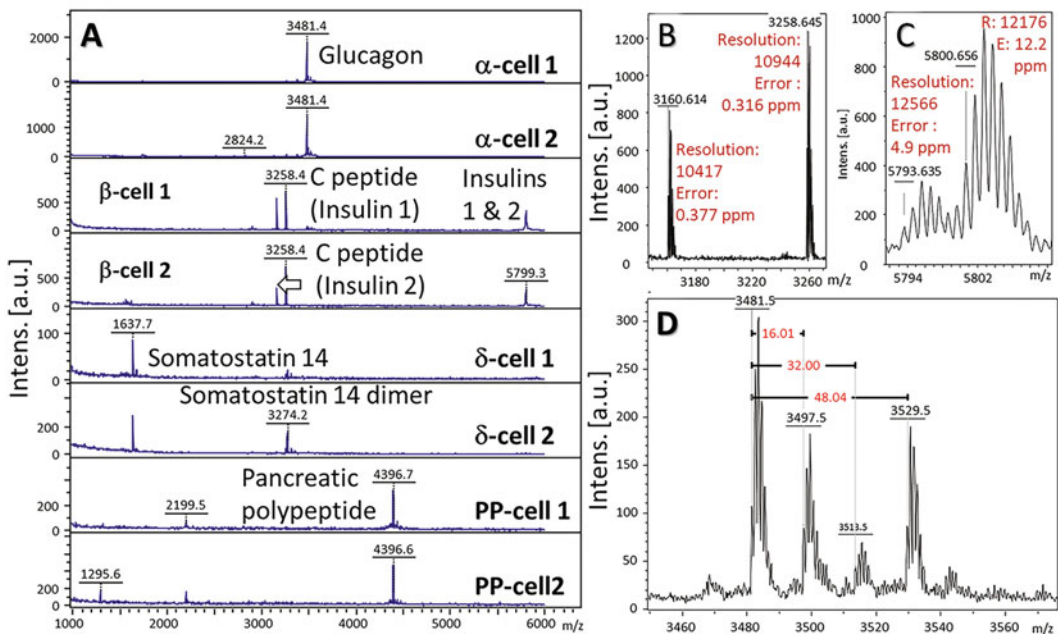


**Fig. 6** Results of microMS-assisted MALDI MS analysis of a single rat pancreatic islet cell population. (a) Examples of mass spectra acquired from eight cells representing main cellular types in the pancreatic islets. (b) Mass spectrum demonstrates insulin 1C and insulin 2C peptide signals with mass resolution and error indicated. (c) Mass spectrum demonstrating insulin 1 and insulin 2 signals with mass resolution and error indicated. (d) Mass spectrum demonstrating putative multiple oxidation of glucagon. Intens. – relative intensity of signals. (a.u.) – arbitrary units. “Error” in ppm is a deviation between the measured mass and the theoretical mass of the selected peak. “Error” is calculated using “SmartFormula Manually” option in flexAnalysis. “Resolution” is mass resolution calculated as part of “Mass list” parameters in flexAnalysis

ppm to single digits (Fig. 6b, c). However, the relative intensity of signals varies between cells. A number of rare observations have included putative multiple oxidation of glucagon (Fig. 6d) and dimerization of somatostatin 14 (Fig. 6a). Both biological and experimental reasons for signal variability should be investigated further.

As mentioned above, image-guided single cell MALDI MS analysis is capable of providing information on the chemical heterogeneity of cellular populations. Proper data processing and analysis are critical for this evaluation. Dispersing a cellular population on an ITO glass surface leads to loss of information on tissue localization, e.g., known localization of  $\beta$ -cells in the islet core surrounded by inhomogeneous layers of  $\alpha$ ,  $\delta$ , and PP cells [69]. Therefore, detected chemical biomarkers are becoming major guiding factors for cell-type determination. Importantly, other approaches for cell-type determination before or after MALDI MS analysis can be used in conjunction with microMS, including immunostaining [36]. Such biomarkers can be predicted using published information or direct data set analysis. As an example, a data set acquired

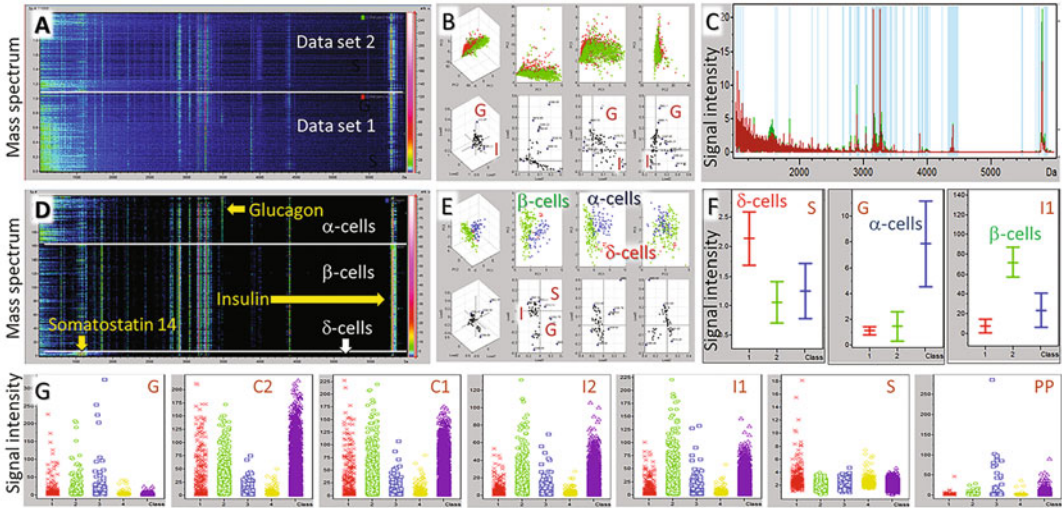


**Fig. 7** Chemical cellular heterogeneity of rat pancreatic islets via microMS-assisted MALDI MS analysis. (a) Gel view of mass spectra acquired from cellular population of a single pancreatic islet divided into two data sets. (b) PCA of the data sets with loading plots demonstrating co-localization of signals related to different cell types, e.g., insulin (I)- and glucagon (G)-expressing cells. (c) Average mass spectrum for both data sets with signals automatically picked by ClinProTools (blue lines). (d) Gel view of filtered and grouped by listed above biomarkers and somatostatin 14 (S) entire set of mass spectra. (e) Results of PCA of three data sets formed by biomarker-guided filtering and grouping of entire set of mass spectra. (f) Histograms of relative intensities of somatostatin 14 (class 1) insulins 1 and 2 (class 2), and glucagon (class 3) signals detected in cells of different types. (g) Distributions of relative signal intensities at  $m/z$  areas of somatostatin 14 (S), glucagon (G), insulin 1 C-peptide (C1), insulin 2 C-peptide (C2), pancreatic polypeptide (PP), insulin 1 (I1), and insulin 2 (I2). These distributions were determined during ClinProTools analysis of mass spectra of cellular populations obtained from five individual rat pancreatic islets (marked on x-axis as class 1–5)

from a cellular population of a single rat pancreatic islet was split into two and evaluated using unsupervised PCA (Fig. 7a–c). Related loading plots revealed compounds that affected the diversity of cellular populations most with Load2 vs. Load3 exhibited two major influences – signals for glucagon and insulin – which were accompanied by other related compounds (Fig. 7b). As expected, score plots did show minor differences between the two populations. Such differences can be important to determine sample inhomogeneity related to experimental or biological factors. Influences of experimental factors, such as gradients in the MALDI matrix layer thickness or localized sample contamination, have to be evaluated to exclude their detrimental effects on measurement results. However, this approach needs further development in terms of cell-to-cell reproducibility (which may be biology-, sample preparation-, or MS measurement-related). Nevertheless, the molecular signatures enable classification of the entire data set into groups related to known cell types (Fig. 7d). This step helps not only to group cells but also to remove cells that exhibit

higher levels of chemical cross-contamination, increasing the reliability of the data analysis. Perhaps dissociation of islets into single cell populations may coincide with loss of cell integrity and release of intracellular analytes. This is noticed when mixed mass spectra are acquired. In such mass spectra, characteristic molecular peaks for distinct cell types may co-localize. As an example, a weak insulin signal is observed in  $\alpha$  cells (orders of magnitude weaker than in  $\beta$  cells), but insulin is not observed in  $\delta$  cells (Fig. 7d). Reanalyzing grouped data sets by supervised PCA demonstrated expected separation of three cell types and provided more information on association of unidentified signals with known cell types (Fig. 7e). Additional statistical output on all associated molecules can be generated (Fig. 7f). Extension of image-guided MALDI MS analysis to cellular populations of different pancreatic islets demonstrates the variability of their cellular composition (Fig. 7g). As expected, the frequency of detection of  $\beta$  cell-related biomarkers, such as insulins 1 and 2, as well as their C peptides, is highest in all five examined islets. However, only one islet demonstrated cells with strong somatostatin 14 signals, and another islet exhibited a large number of insulin-producing cells but a small number of glucagon-expressing cells. Ratios of relative intensities for insulin 1/insulin 1C peptide and insulin 2/insulin 2C peptide are similar for each of the examined pancreatic islets, which is indicative of good repeatability of measurements. These results corroborate well with previous findings on the cellular heterogeneity of pancreatic islets [69, 70]. We expect similar results are possible on many other cell types.

---

## Acknowledgments

The authors gratefully acknowledge support from the American Diabetes Association Pathway award number 1-18-VSN-19, the National Institute on Drug Abuse award number P30 DA018310, and the National Institute of Mental Health, award number 1 U01 MH109062. microMS was designed and programmed by Dr. Troy J. Comi. Dr. Elizabeth K. Neumann and Dr. Thanh D. Do made significant contributions in the development and application of microMS. Dr. Ali Naji and Dr. Chengyang Liu (Division of Transplantation, Department of Surgery, Hospital of the University of Pennsylvania, Philadelphia, PA) provided live isolated human islets for this project. We thank Dan Castro for valuable comments.

## References

1. Hooke R (1665) *Micrographia* or, some physiological descriptions of minute bodies made by magnifying glasses: with observations and inquiries thereupon. J. Martyn and J. Allestry, London
2. Comi TJ, Do TD, Rubakhin SS et al (2017) Categorizing cells on the basis of their chemical profiles: progress in single-cell mass Spectrometry. *J Am Chem Soc* 139(11):3920–3929. <https://doi.org/10.1021/jacs.6b12822>
3. Neumann EK, Do TD, Comi TJ et al (2019) Exploring the fundamental structures of life: non-targeted, chemical analysis of single cells and subcellular structures. *Angew Chem Int Ed Engl* 58(28):9348–9364. <https://doi.org/10.1002/anie.201811951>
4. Dey S (2018) *Hands-on image processing with python: expert techniques for advanced image analysis and effective interpretation of image data*. Packt Publishing Ltd, Birmingham
5. Prasad S, Chanussot J (eds) (2020) *Hyperspectral image analysis: advances in machine learning and signal processing*. Springer International Publishing, Switzerland AG. <https://doi.org/10.1007/978-3-030-38617-7>
6. Umbaugh SE (2017) *Digital image processing and analysis: applications with MATLAB and CVIPtools*. CRC Press, Boca Raton
7. Klaus DT (2017) *Guide to medical image analysis: methods and algorithms*. Springer, London. <https://doi.org/10.1007/978-1-4471-7320-5>
8. Fu AY, Spence C, Scherer A et al (1999) A microfabricated fluorescence-activated cell sorter. *Nat Biotechnol* 17(11):1109–1111. <https://doi.org/10.1038/15095>
9. Hawley TS, Hawley RG (eds) (2017) *Flow cytometry protocols*, 4th edn. Springer, New York
10. Blasco J, Cubero S, Gomez-Sanchis J et al (2009) Development of a machine for the automatic sorting of pomegranate (*Punica granatum*) arils based on computer vision. *J Food Eng* 90(1):27–34. <https://doi.org/10.1016/j.jfoodeng.2008.05.035>
11. Cheng Y, Jafari MA (2008) Vision-based online process control in manufacturing applications. *IEEE Trans Autom Sci Eng* 5(1):140–153. <https://doi.org/10.1109/Tase.2007.912058>
12. Huang SH, Pan YC (2015) Automated visual inspection in the semiconductor industry: a survey. *Comput Ind* 66:1–10. <https://doi.org/10.1016/j.compind.2014.10.006>
13. Jardini AL, Larosa MA, Maciel R et al (2014) Cranial reconstruction: 3D biomodel and custom-built implant created using additive manufacturing. *J Cranio Maxill Surg* 42(8):1877–1884. <https://doi.org/10.1016/j.jcms.2014.07.006>
14. Jannin P, Fitzpatrick JM, Hawkes DJ et al (2002) Validation of medical image processing in image-guided therapy. *Ieee Trans Med Imaging* 21(12):1445–1449. <https://doi.org/10.1109/Tmi.2002.806568>
15. Zhang QC, Yang LT, Chen ZK et al (2018) A survey on deep learning for big data. *Inform Fusion* 42:146–157. <https://doi.org/10.1016/j.inffus.2017.10.006>
16. Urban PL, Jefimovs K, Amantonico A et al (2010) High-density micro-arrays for mass spectrometry. *Lab Chip* 10(23):3206–3209. <https://doi.org/10.1039/c0lc00211a>
17. Ibanez AJ, Svatos A (2020) Applications of MicroArrays for Mass Spectrometry (MAMS) in single-cell metabolomics. *Methods Mol Biol* 2064:73–88. [https://doi.org/10.1007/978-1-4939-9831-9\\_6](https://doi.org/10.1007/978-1-4939-9831-9_6)
18. Yang T, Gao D, Jin F et al (2016) Surface-printed microdot array chips coupled with matrix-assisted laser desorption/ionization mass spectrometry for high-throughput single-cell patterning and phospholipid analysis. *Rapid Commun Mass Spectrom* 30(Suppl 1):73–79. <https://doi.org/10.1002/rcm.7628>
19. Zimmermann M, Escrig S, Hubschmann T et al (2015) Phenotypic heterogeneity in metabolic traits among single cells of a rare bacterial species in its natural environment quantified with a combination of flow cell sorting and NanoSIMS. *Front Microbiol* 6:243. <https://doi.org/10.3389/fmicb.2015.00243>
20. Zimmerman TA, Rubakhin SS, Sweedler JV (2011) MALDI mass spectrometry imaging of neuronal cell cultures. *J Am Soc Mass Spectrom* 22(5):828–836. <https://doi.org/10.1007/s13361-011-0111-2>
21. Schober Y, Guenther S, Spengler B et al (2012) Single cell matrix-assisted laser desorption/ionization mass spectrometry imaging. *Anal Chem* 84(15):6293–6297. <https://doi.org/10.1021/ac301337h>
22. Spitzer MH, Nolan GP (2016) Mass cytometry: single cells, many features. *Cell* 165(4):780–791
23. Wu H, Volponi JV, Oliver AE et al (2011) In vivo lipidomics using single-cell Raman spectroscopy. *Proc Natl Acad Sci U S A* 108(9):3809–3814

24. Baker MJ, Trevisan J, Bassan P et al (2014) Using Fourier transform IR spectroscopy to analyze biological materials. *Nat Protoc* 9(8): 1771
25. Bolognesi MM, Manzoni M, Scalia CR et al (2017) Multiplex staining by sequential immunostaining and antibody removal on routine tissue sections. *J Histochem Cytochem* 65(8): 431–444. <https://doi.org/10.1369/0022155417719419>
26. Dixon AR, Bathany C, Tsuei M et al (2015) Recent developments in multiplexing techniques for immunohistochemistry. *Expert Rev Mol Diagn* 15(9):1171–1186. <https://doi.org/10.1586/14737159.2015.1069182>
27. Lanni EJ, Rubakhin SS, Sweedler JV (2012) Mass spectrometry imaging and profiling of single cells. *J Proteome* 75(16):5036–5051. <https://doi.org/10.1016/j.jprot.2012.03.017>
28. Li L, Garden RW, Sweedler JV (2000) Single-cell MALDI: a new tool for direct peptide profiling. *Trends Biotechnol* 18(4):151–160. [https://doi.org/10.1016/s0167-7799\(00\)01427-x](https://doi.org/10.1016/s0167-7799(00)01427-x)
29. Chen R, Li L (2010) Mass spectral imaging and profiling of neuropeptides at the organ and cellular domains. *Anal Bioanal Chem* 397(8): 3185–3193. <https://doi.org/10.1007/s00216-010-3723-7>
30. Ong TH, Kissick DJ, Jansson ET et al (2015) Classification of large cellular populations and discovery of rare cells using single cell matrix-assisted laser desorption/ionization time-of-flight mass Spectrometry. *Anal Chem* 87(14): 7036–7042. <https://doi.org/10.1021/acs.analchem.5b01557>
31. Do TD, Comi TJ, Dunham SJ et al (2017) Single cell profiling using ionic liquid matrix-enhanced secondary ion mass Spectrometry for neuronal cell type differentiation. *Anal Chem* 89(5):3078–3086. <https://doi.org/10.1021/acs.analchem.6b04819>
32. Jansson ET, Comi TJ, Rubakhin SS et al (2016) Single cell peptide heterogeneity of rat islets of Langerhans. *ACS Chem Biol* 11(9): 2588–2595. <https://doi.org/10.1021/acscchembio.6b00602>
33. Comi TJ, Neumann EK, Do TD et al (2017) microMS: a python platform for image-guided mass Spectrometry profiling. *J Am Soc Mass Spectrom* 28(9):1919–1928. <https://doi.org/10.1007/s13361-017-1704-1>
34. Comi TJ, Makurath MA, Philip MC et al (2017) MALDI MS guided liquid microjunction extraction for capillary electrophoresis-electrospray ionization MS analysis of single pancreatic islet cells. *Anal Chem* 89(14): 7765–7772. <https://doi.org/10.1021/acs.analchem.7b01782>
35. Choe K, Xue P, Zhao H et al (2021) macroMS: image-guided analysis of random objects by matrix-assisted laser desorption/ionization time-of-flight mass spectrometry. *J Am Soc Mass Spectrom* 32(5):1180–1188. <https://doi.org/10.1021/jasms.1c00013>
36. Neumann EK, Comi TJ, Rubakhin SS et al (2019) Lipid heterogeneity between astrocytes and neurons revealed by single-cell MALDI-MS combined with Immunocytochemical classification. *Angew Chem Int Ed Engl* 58(18): 5910–5914. <https://doi.org/10.1002/anie.201812892>
37. DiPeso L, Ji DX, Vance RE et al (2017) Cell death and cell lysis are separable events during pyroptosis. *Cell Death Discov* 3. <https://doi.org/10.1038/cddiscovery.2017.70>
38. Do TD, Ellis JF, Neumann EK et al (2018) Optically guided single cell mass Spectrometry of rat dorsal root ganglia to profile lipids, peptides and proteins. *ChemPhysChem* 19(10): 1180–1191. <https://doi.org/10.1002/cphc.201701364>
39. Castro DC, Xie YR, Rubakhin SS et al (2021) Image-guided MALDI mass Spectrometry for high-throughput single-organelle characterization. *Nat Methods* 18:1233–1238
40. Villarreal D, Pradhan G, Wu CS et al (2019) A simple high efficiency protocol for pancreatic islet isolation from mice. *J Vis Exp* 150. <https://doi.org/10.3791/57048>
41. Berman ES, Fortson SL, Checchi KD et al (2008) Preparation of single cells for imaging/profiling mass spectrometry. *J Am Soc Mass Spectrom* 19(8):1230–1236. <https://doi.org/10.1016/j.jasms.2008.05.006>
42. Batoy SMAB, Akhmetova E, Miladinovic S et al (2008) Developments in MALDI mass spectrometry: the quest for the perfect matrix. *Appl Spectrosc Rev* 43(6):485–550. <https://doi.org/10.1080/05704920802108198>
43. Hankin JA, Barkley RM, Murphy RC (2007) Sublimation as a method of matrix application for mass spectrometric imaging. *J Am Soc Mass Spectrom* 18(9):1646–1652. <https://doi.org/10.1016/j.jasms.2007.06.010>
44. Yang J, Caprioli RM (2011) Matrix sublimation/recrystallization for imaging proteins by mass spectrometry at high spatial resolution. *Anal Chem* 83(14):5728–5734. <https://doi.org/10.1021/ac200998a>
45. Gemperline E, Rawson S, Li L (2014) Optimization and comparison of multiple MALDI matrix application methods for small molecule mass spectrometric imaging. *Anal Chem*



- 86(20):10030–10035. <https://doi.org/10.1021/ac5028534>
46. Meechan PJ, Potts J (eds) (2020) Biosafety in microbiological and biomedical laboratories, 6th edn. Center for Disease Control and Prevention; National Institutes of Health, <https://www.cdc.gov/labs/BMBL.html>
  47. Capicciotti CJ, Kurach JD, Turner TR et al (2015) Small molecule ice recrystallization inhibitors enable freezing of human red blood cells with reduced glycerol concentrations. *Sci Rep* 5:9692. <https://doi.org/10.1038/srep09692>
  48. Carter JD, Dula SB, Corbin KL et al (2009) A practical guide to rodent islet isolation and assessment. *Biol Proced Online* 11:3–31. <https://doi.org/10.1007/s12575-009-9021-0>
  49. Corbin KL, West HL, Brodsky S et al (2021) A practical guide to rodent islet isolation and assessment revisited. *Biol Proced Online* 23(1):7. <https://doi.org/10.1186/s12575-021-00143-x>
  50. Neuman JC, Truchan NA, Joseph JW et al (2014) A method for mouse pancreatic islet isolation and intracellular cAMP determination. *J Vis Exp* 88:e50374. <https://doi.org/10.3791/50374>
  51. bigTIFF (2021) <http://bigtiff.org/>
  52. OpenSlide (2021) <https://openslide.org/>
  53. Goode A, Gilbert B, Harkes J et al (2013) OpenSlide: a vendor-neutral software foundation for digital pathology. *J Pathol Inform* 4:27. <https://doi.org/10.4103/2153-3539.119005>
  54. Bugovsky S, Winkler W, Balika W et al (2015) Long time storage (archiving) of peptide, protein and tryptic digest samples on disposable nano-coated polymer targets for MALDI MS. *EuPA Open Proteom* 8:48–54. <https://doi.org/10.1016/j.euprot.2015.07.013>
  55. Romanova EV, Rubakhin SS, Sweedler JV (2008) One-step sampling, extraction, and storage protocol for peptidomics using dihydroxybenzoic acid. *Anal Chem* 80(9):3379–3386. <https://doi.org/10.1021/ac7026047>
  56. Malys BJ, Piotrowski ML, Owens KG (2018) Diagnosing and correcting mass accuracy and signal intensity error due to initial ion position variations in a MALDI TOFMS. *J Am Soc Mass Spectrom* 29(2):422–434. <https://doi.org/10.1007/s13361-017-1845-2>
  57. Christian NP, Arnold RJ, Reilly JP (2000) Improved calibration of time-of-flight mass spectra by simplex optimization of electrostatic ion calculations. *Anal Chem* 72(14):3327–3337. <https://doi.org/10.1021/ac991500h>
  58. Barry JA, Robichaud G, Muddiman DC (2013) Mass recalibration of FT-ICR mass spectrometry imaging data using the average frequency shift of ambient ions. *J Am Soc Mass Spectrom* 24(7):1137–1145. <https://doi.org/10.1007/s13361-013-0659-0>
  59. Mass spectrometry data format (2021) [https://en.wikipedia.org/wiki/Mass\\_spectrometry\\_data\\_format](https://en.wikipedia.org/wiki/Mass_spectrometry_data_format)
  60. Mass Spectrometry and Bioanalytics (2021) <https://www.mathworks.com/help/bioinfo/mass-spectrometry-and-bioanalytics.html>
  61. Norris JL, Cornett DS, Mobley JA et al (2007) Processing MALDI mass spectra to improve mass spectral direct tissue analysis. *Int J Mass Spectrom* 260(2–3):212–221. <https://doi.org/10.1016/j.ijms.2006.10.005>
  62. McDonnell LA, van Remoortere A, de Velde N et al (2010) Imaging mass spectrometry data reduction: automated feature identification and extraction. *J Am Soc Mass Spectrom* 21(12):1969–1978. <https://doi.org/10.1016/j.jasms.2010.08.008>
  63. UniProt (2021) <https://www.uniprot.org/>
  64. Consortium TU (2020) UniProt: the universal protein knowledgebase in 2021. *Nucleic Acids Res* 49(D1):D480–D489. <https://doi.org/10.1093/nar/gkaa1100>
  65. NCBI > Proteins > Protein Database (2021). <https://www.ncbi.nlm.nih.gov/protein>
  66. Yates JR 3rd, Speicher S, Griffin PR et al (1993) Peptide mass maps: a highly informative approach to protein identification. *Anal Biochem* 214(2):397–408. <https://doi.org/10.1006/abio.1993.1514>
  67. Henzel WJ, Billeci TM, Stults JT et al (1993) Identifying proteins from two-dimensional gels by molecular mass searching of peptide fragments in protein sequence databases. *Proc Natl Acad Sci U S A* 90(11):5011–5015. <https://doi.org/10.1073/pnas.90.11.5011>
  68. Pappin DJ, Hojrup P, Bleasby AJ (1993) Rapid identification of proteins by peptide-mass fingerprinting. *Curr Biol* 3(6):327–332. [https://doi.org/10.1016/0960-9822\(93\)90195-t](https://doi.org/10.1016/0960-9822(93)90195-t)
  69. Cabrera O, Berman DM, Kenyon NS et al (2006) The unique cytoarchitecture of human pancreatic islets has implications for islet cell function. *Proc Natl Acad Sci U S A* 103(7):2334–2339. <https://doi.org/10.1073/pnas.0510790103>
  70. Pisanía A, Weir GC, O’Neil JJ et al (2010) Quantitative analysis of cell composition and purity of human pancreatic islet preparations. *Lab Invest* 90(11):1661–1675. <https://doi.org/10.1038/labinvest.2010.124>